Report No. P-10

CRITICAL MEASUREMENTS ON EARLY MISSIONS TO JUPITER

by

J. M. Witting
M. W. P. Cann
T. C. Owen

Astro Sciences Center

of

IIT Research Institute
Chicago, Illinois

for

Lunar and Planetary Programs
Office of Space Science and Applications
NASA Headquarters
Washington, D. C.

Contract No. NASr-65(06)

APPROVED:

C. A. Stone, Director
Astro Sciences Center

December 1965

IIT RESEARCH INSTITUTE

SUMMARY

Existing knowledge of Jupiter's magnetosphere, ionosphere, atmosphere, and interior is summarized, and critical measurements which can be made from fly-by missions to Jupiter are indicated.

Studies of radio emission have indicated the presence of a sizable magnetic moment and radiation belts of energetic electrons. Estimates place Jupiter's surface magnetic field strength at about 10 gauss, and indicate the presence of radiation belts, similar to the Earth's in configuration, but with particle densities about 1000 times greater than the Earth's. These estimates are probably correct to within an order of magnitude. The magnetosphere extends to at least 40 Jupiter radii at the subsolar point.

The presence of an ionosphere has been deduced theoretically, assuming a model atmosphere. Primarily because of lower solar radiation flux and smaller recombination cross sections, the theories predict lower ionization and recombination rates on Jupiter than on Earth. The resulting concentrations of electrons are estimated to peak at about 10^6 electrons/cm^3 at about 200 km above the cloud tops.

Three constituents have been identified in Jupiter's atmosphere by spectral observation. Hydrogen is known to be present in large quantities though the actual amount of hydrogen is quite uncertain at present. Amounts of methane (150 meter atmospheres) and ammonia (7 meter atmospheres) are small. Based on cosmic abundance arguments, large amounts of helium should also be present, with smaller amounts of neon.

The temperature in the Jovian atmosphere has been measured at various wavelengths in the microwave and infrared regions of the spectrum. The temperatures obtained ($\simeq$ 150°K) are somewhat higher than the blackbody temperature for the planet (93°K - 131°K). They fluctuate over a range from 125°K to 200°K in the wavelength range 8μ to 3 cm, indicating that the observed thermal emission at the different wavelengths comes from different depths in the atmosphere.

Model studies of Jupiter's interior have indicated the possible presence of metallic hydrogen and a high density core near the center of the planet. Large errors may be present in calculated densities, because of the lack of knowledge of the equation of state for hydrogen and helium under pressures calculated (up to 10^7 atmospheres), which lie above terrestrial measurements (up to 2×10^4 atmospheres).

The magnetosphere, atmosphere, and interior of Jupiter are of primary scientific interest at this time. Although properties of the magnetosphere and atmosphere can be measured relatively directly by a spacecraft, the interior is

inaccessible to direct measurements. Useful gains in knowledge of the interior are possible, however, from inferences that can be drawn from a better knowledge of the magnetosphere and atmosphere. Eleven measurements which are feasible now or in the near future are suggested for early missions to Jupiter. Most are directly concerned with Jupiter's magnetosphere or atmosphere. Parameters measured would be: 1) magnetic field strength and orientation, 2) flux of 40 kev electrons, 3) flux of relativistic electrons, 4) flux of energetic protons, 5) atmospheric and ionospheric scale heights, 6) ionospheric electron density profiles, 7) emission spectra from 1000-7000 Å, 8) H, He, and Ne line strengths under high resolution, 9) temperature at 10-13μ, 10) temperature at 7 mm, and 11) polarization of reflected sunlight.

It is concluded that:

1. A modest number of experiments carried out on a spacecraft fly-by mission to Jupiter can significantly add to present knowledge.
2. The distance of closest approach to Jupiter can be quite large, up to 40 R_J, for significant yields from some of the most important experiments. For magnetospheric studies, step functions in information level occur for penetration within 6 R_J and within 3 R_J.
3. Trajectory requirements for a particularly desirable mission are quite reasonable, requiring an ideal velocity of 54,000 ft/sec and a time of flight from Earth to Jupiter of 500 days.

TABLE OF CONTENTS

TABLE OF CONTENTS (Cont'd)

LIST OF TABLES

LIST OF FIGURES

Report No. P-10

CRITICAL MEASUREMENTS ON EARLY MISSIONS TO JUPITER

1. INTRODUCTION

The primary attraction of Jupiter as an object of scientific investigation is that the Jovian planets are very different from the terrestrial planets with which we are somewhat familiar. Jupiter and the other giant planets are characterized by their large masses and low densities. The mass of Jupiter is equal to 318 Earth masses; the smallest known star is only 16 times more massive than Jupiter. Yet the mean density of Jupiter is only 1.3 gm/cm^3, compared with 5.5 gm/cm^3 for the Earth.

It is generally assumed that these differences can be interpreted in terms of basic differences in the evolution of the planets since the time of their formation. In this view, it is suggested that the atmospheres of the terrestrial planets are secondary, having been produced by outgassing after the primitive atmospheres were dissipated. The Jovian planets, however, are thought to retain a large fraction of their

primitive atmospheres, with roughly the same relative composition suggested by the cosmic abundance of the elements. Since hydrogen and helium are the most abundant elements, the low mean densities of these planets can easily be explained. Present observational data appear to support this view. Thus an examination of Jupiter permits us to study the lighter fraction of the elements that were available for formation of the planets in roughly their original relative abundances.

In addition to this basic reason for interest in Jupiter, the planet presents a fascinating array of puzzling phenomena, most of which are only imperfectly understood. As an example, Earth, Jupiter, and possibly Saturn have radiation belts and substantial magnetic fields, while Mars and Venus do not. To explain this basic similarity amidst such basic differences is a challenge in any attempt at a comprehensive understanding of the solar system.

The purpose of this report is to review the most recent observations and theories about various Jovian phenomena and their relationship to the slowly emerging picture of the basic structure of Jupiter. Section 2 discusses what kinds of spacecraft experiments will best supplement our present knowledge and resolve the differences in current theories of Jupiter. Interestingly, a rather simple low-energy mission to Jupiter is capable of yielding valuable information. Section 3 is a detailed discussion of those aspects of Jupiter which were considered in this study.

It is anticipated that much of the material presented will be out of date within a few years, since considerable attention is being devoted to Jupiter and information is bound to accumulate at a rapid rate. Nevertheless, some of the material and some of the suggested trends in thinking will remain valid even as more data become available.

2. CRITICAL MEASUREMENTS AND THEIR INFLUENCE ON FLY-BY MISSIONS TO JUPITER

Much information about Jupiter has been obtained from ground-based observations, but more critical information can be obtained most appropriately from spacecraft missions to Jupiter. Some critical measurements that can significantly aid our understanding of Jupiter are summarized here. A selected set of trajectories is included, since the choice of a trajectory influences many of the measurements. The reasoning leading to the choice of measurements is amplified in Section 3.

2.1 Measurements

Table 1 lists some of the most important measurements to be made on early fly-by missions to Jupiter. Included in the table are ranges, possible instruments, maximum desired distance of closest approach, lighting conditions, and the reference to the more complete discussion in Section 3.

Table 1

MEASUREMENTS FROM SPACECRAFT

Expt. No.	Measurement	Range	Possible Instrument	Maximum Closest Approach for Useful Output	Side of Jupiter (+ sunlight - dark o irrelevant)	Location of Discussion
1.	Magnetic field	1/2γ - 10G (2.5 R_J) 1G (5 R_J) 500γ (25 R_J)	Magnetometer	40 R_J	+,-	3.1
2.	Flux of 40-kev electrons	10^9-10^{13}/cm^{2}sec kev	Counter	6	+,-	3.1
3.	Flux of relativistic electrons	10^4-10^6/cm^{2}sec mev	Counter	3	o	3.1
4.	Flux of energetic protons	10^8-10^{11}/cm^{2}sec	Counter	3	o	3.1
5.	Atmospheric & ionospheric scale heights	30-50 Mc;10,000 Mc	Occultation of telemetry or other radio signals	40	+,-	3.2; 3.3 3.5
6.	Ionospheric electron density; collision frequency	3-30 Mc	Ionosonde	3	+,-	3.5
7.	Several emission lines, scanning in λ with resolution to 5000	1000-7000 Å	Ultraviolet spectro-photometer	40	+,-	3.2
8.	H, He, Ne lines, resolving parts of planet	1216Å(H);3888Å(He); 6402Å(Ne), optics resolution ~1/2° of arc	Ultraviolet photometer	6	+,-	3.2
9.	Temperature high in atmosphere from 10-13 λ, resolving parts of planet	100-225°K	Far-infrared radiometer	3	+,-	3.3
10.	Temperature low in atmosphere at 0.7 mm	100-225°K	Radiometer	3	+,-	3.3
11.	Polarization of reflected sunlight in visible and infrared	Polarization:	Photometric polarimeter	40	+	3.4

Experiment 1 - Magnetic Field

Of the planets and satellites that have been studied by spacecraft - Earth, moon, Venus, Mars - only Earth is known to have a substantial magnetic field and a resulting magnetosphere. Jupiter also has a substantial magnetosphere, the details of which can best be studied by a mission to the vicinity of the planet.

Some knowledge of Jupiter's magnetosphere has been obtained from Earth-based observations of radio emission. In particular, it is known that a large magnetic field, estimated to be of the order of 10 gauss at the surface, surrounds Jupiter. Jupiter's magnetosphere extends about forty Jupiter radii from its center (40 R_J) toward the Sun and farther in other directions.

Large numbers of relativistic electrons almost certainly form a radiation belt from $L_J = 2$ to $L_J = 3$, $L_J = N$ being a field line having (magnetic) equatorial distance N Jupiter radii from the (magnetic) center of Jupiter. For $L_J > 2$, a position on the (rotational) equatorial plane at R_J has $L_J \sim R_J$, the effects of off-centered and slightly skew magnetic moments leading to only small differences.

The magnitude of Jupiter's magnetic moment is uncertain to an order of magnitude or two. Its configuration, i.e., whether dipole or not, and, if so, the location of the dipole center, are speculative. Its extent (the size of the magnetosphere) is better known. However, the interactions

with the solar wind probably lead to a standoff shock wave and a turbulent transition region between the shock and the magnetosphere and they are not capable of examination from Earth.

Measurements of the magnetic field along the spacecraft's trajectory can considerably improve present knowledge of the size and the configuration of Jupiter's field. A rubidium vapor magnetometer of the type flown on IMP I is suitable for the weak fields ($1/2\gamma$ to 60γ) in the outer portion of the magnetosphere. For measurements closer to Jupiter extension of the range to the higher field strengths shown in Table 1, or inclusion of a second instrument will be necessary.

Minimum trajectory requirements are that the spacecraft enter Jupiter's magnetosphere, which is expected to occur beyond 40 R_J.

Experiment 2 - Moderate-Energy Electrons

The origin of decameter radio emission from Jupiter is not well understood, though many theories have been proposed. It is known that the planetary satellite Io at 6 R_J is involved. If the emission mechanism were understood, the vast amount of data on decameter emission could be used to study numerous time-dependent processes occurring in Jupiter's magnetosphere.

The key to interpreting the decameter emission may be a measurement of the fluxes of moderately energetic (10 to 100 kev) electrons in the vicinity of the orbit of Io, since the two most widely accepted theories both require the existence of such electrons. The counters flown on Injun III, but

modified to handle the larger fluxes per unit energy interval of 10^9 to 10^{13} per square centimeter per second per kev (19^9-10^{13}/cm^2 sec kev) anticipated for Jupiter, are suitable.

The trajectory requirement is that the measurements be made near 6 R_J and less.

Experiment 3 - Relativistic Electrons

Decimeter emission indicates a belt of relativistic electrons at 2 to 3 R_J. Chang and Davis (1962) have reported a relation between observed radiation and density of energetic electrons, size of radiating region, and magnetic field. Direct measurement of the flux of relativistic electrons can yield the density and the size. Thus, in addition to providing direct knowledge of the radiation belt properties, the inferred magnetic field magnitude can be compared with a direct measurement.

With modification, the University of Chicago counter flown on IMP I is probably suitable for measuring fluxes of high-energy electrons in the range of 10^4 to 10^6/cm^2 sec mev.

The spacecraft should penetrate to within 3 R_J near the equatorial plane in order to get into the radiation belt.

Experiment 4 - Energetic Protons

Present knowledge neither affirms nor negates that an energetic proton radiation belt like Earth's exists near Jupiter. Since such a belt might present a hazard to future missions going near Jupiter, it is important that early missions seek to determine whether it exists.

Measurement of fluxes of energetic protons can be useful in finding a radiation belt. Energetic proton detectors

having various flux ranges have been flown in many spacecraft, so the preparation of a counter sensitive to > 30 mev protons over the desired range of 10^8 to $10^{11}/cm^2$ sec should present no difficulty.

In analogy with Earth's inner Van Allen belt, any proton belt might be expected to be rather close to the planet. Therefore, to obtain useful information, the spacecraft should come within 3 R_J.

Experiment 5 - Occultation

A quantity of considerable interest in the analysis of planetary atmospheres and ionospheres is the scale height at a given elevation. The atmospheric scale height is the distance over which the atmospheric density changes by a factor 1/e. The ionospheric scale height is the distance over which the electron changes by a factor 1/e.

The scale height of Jupiter's atmosphere was measured by Baum and Code (1953), who observed an occultation of a star by the planet. It would be of great value to repeat this measurement from a spacecraft, however, particularly if the atmospheric temperature were measured simultaneously. If it is possible to determine the temperature at the atmospheric level at which the scale height is determined which might be obtainable from the occultation data, the molecular weight could also be determined.

The presence of a Jovian ionosphere has been predicted on Jupiter from deductions based on decameter radio emission and from photochemical reactions expected. Such an ionosphere

could be of major interest in planning communications for later spacecraft missions and in understanding the physical and photochemical processes taking place in the atmosphere. If radio frequencies are used during the occultation, the ionospheric scale height can be measured.

An occultation experiment of this nature has already been successfully carried out for the Martian atmosphere and ionosphere from Mariner IV. The observations were made with an S-band signal (2300 Mc). This frequency will probably not be appropriate for a Jupiter experiment, because of strong interference from the electron radiation belt. It will be necessary to use a frequency at which the intensity of the radio signal emanating from the planet itself can be overcome. Frequencies near 10,000 Mc can be used to measure atmospheric scale height. Frequencies from 30 to 50 Mc are necessary if the ionospheric scale height are also desired.

Trajectory requirements are minimal; a 40 R_J minimum approach is satisfactory.

Experiment 6 - Ionosphere

A more sophisticated ionospheric experiment is a topside ionosonde, which is capable of determining a profile of the electron density above the region of maximum density. Theoretical values currently range from 10^5 to 10^7 electrons/cm^3. For an electron density range of 10^5 to $10^7/cm^3$, a frequency range of 3 to 30 Mc is required. There is a current NASA topside ionosonde program in which such measurements have been made from orbiting satellites at frequencies in the proper range

In order to be effective, a relatively close approach, $< 3\ R_J$, must be made.

Experiment 7 - Overall Composition

Methane, ammonia, and hydrogen are known to exist in the atmosphere of Jupiter, although the amount of hydrogen is known to no better than an order of magnitude.

Arguments based on the cosmic abundance of the elements suggest the presence, in addition, of a large amount of helium and small quantities of neon and argon. The photochemical reactions expected in an atmosphere of this composition suggest traces of other constituents, e.g., ethane. It has not been possible to verify the presence of any of these elements primarily because the ultraviolet region of the spectrum is inaccessible to ground-based observations.

The presence of trace constituents and the amount of hydrogen can be determined from a suitably equipped spacecraft. The ultraviolet spectrum could be examined without interference from Earth's upper atmosphere. More importantly, a fly-by passing behind the planet would permit detection of the emission spectrum from the dark side, rather than the reflection spectrum now observed from Earth. The required instrumentation is a spectrophotometer of the type already considered for the Mars Mariner series. The spectral range should be 1000 to 7000 Å, with variable resolution ($\Delta\lambda/\lambda$) to a maximum of 5000.

Since only the entire planet need be resolved, measurements at 40 R_J or less will be satisfactory, although better spatial resolution would be desirable.

Experiment 8 - Detailed Spectra

The spectrophotometer employed for Experiment 7 can also be employed as a photometer by setting it at a fixed wavelength. With a suitable optical system one can scan over the disk and variations in the concentration of a given constituent can be detected. The suggested wavelengths are 1216 Å, for detecting hydrogen; 3888 Å, for helium; and 6402 Å, for neon.

Since high spatial resolution is desired, a relatively close approach, $< 6\ R_J$, is required.

Experiment 9 - Infrared Temperature

The variation of Jovian temperature with depth is a function of the atmospheric opacity, which at present is not well known. Any discussion of the thermal history of the planet depends on knowledge of the way in which the atmosphere affects the transfer of radiation. It is therefore of great interest to obtain temperature measurements at a variety of wavelengths, which can be roughly related to the depth at which the thermal emission occurs. Preferably high angular resolution should be used, so that isotherms can be drawn over the disk of the planet and compared with visual features.

Such work has been initiated by means of ground-based observations through the 8 to 14μ atmospheric window. However, the available instrumentation must be modified for inclusion in a spacecraft. The instrument should be capable of detecting temperature differences of 0.5°K over a range from 1000 to 225°K. A detailed scan of the disk in the 10 to 13μ region, including observations of the dark side, is suggested. This will extend

the angular resolution obtained from the ground, will permit determination of cooling rates, and will facilitate correlation of ground-based and fly-by measurements.

A relatively close approach, $< 3\ R_J$, is required to justify this sensitivity and to obtain the desired spatial resolution.

Experiment 10 - Radio Temperature

A gallium-doped germanium bolometer of the type described by Low (1961) is suggested for detection of infrared emission between 5000 and 1000μ (1 mm). This represents the wavelength interval between the lowest rotational line of ammonia and the highest microwave frequency at which ground-based observations can be made. The observations should be extended to the dark side in order to determine cooling rates over the disk.

As in Experiment 9, a close approach, $< 3\ R_J$, is probably required.

Experiment 11 - Optical Polarization

Polarimetry is one method for determining the physical state of clouds high in Jupiter's atmosphere, since the polarizing properties of a cloud are strongly dependent on particle size and refractive index. From the Earth it is possible to observe only 11° of phase angle, but a spacecraft on a fly-by mission views all phase angles, 0 to 180°. Furthermore, poor seeing, a problem not encountered in spacecraft missions, makes Earth-based measurements difficult.

FIGURE 1

EXAMPLES OF FLY-BY TRAJECTORIES

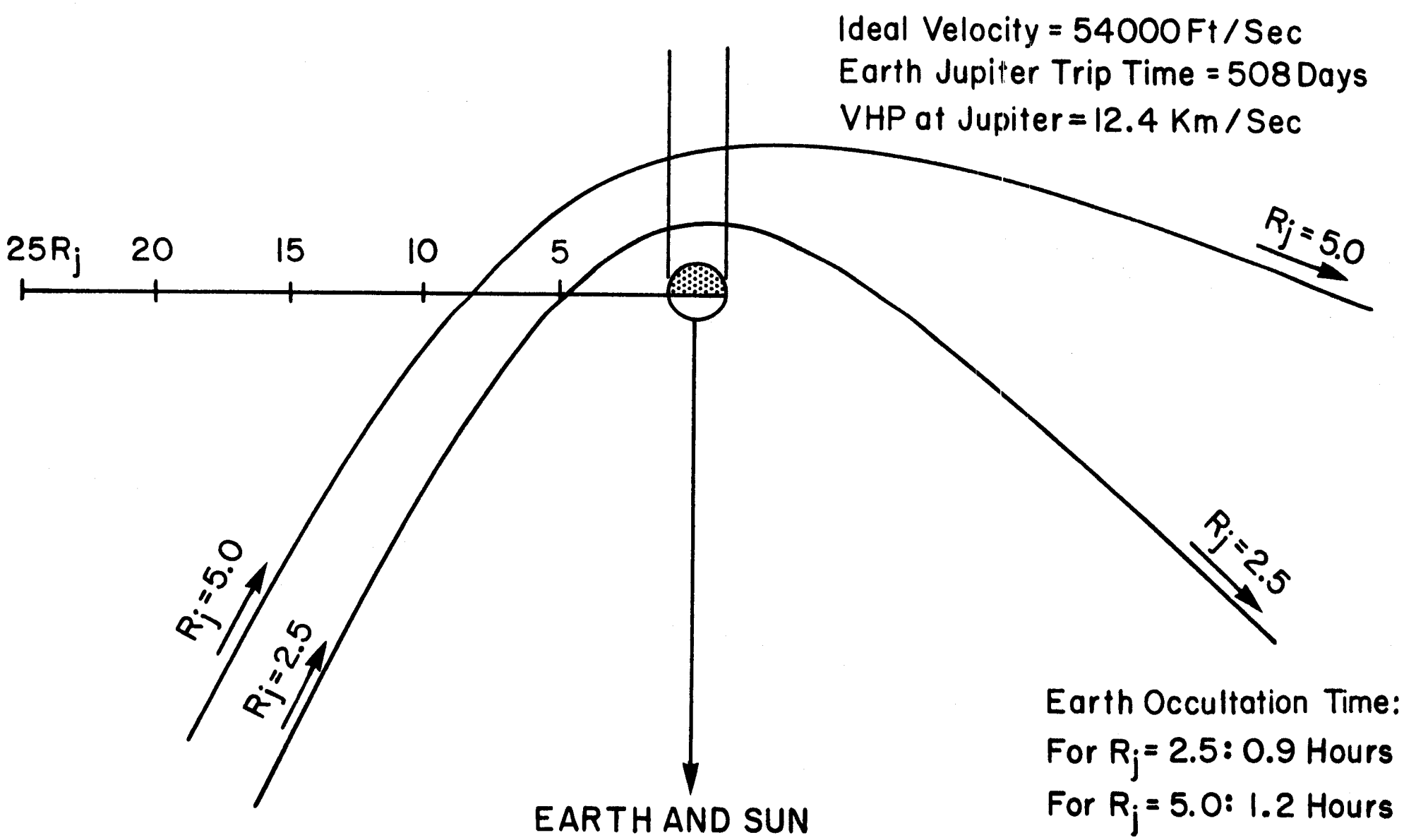

FIGURE 2

EXAMPLES OF POST-JUPITER ORBITS

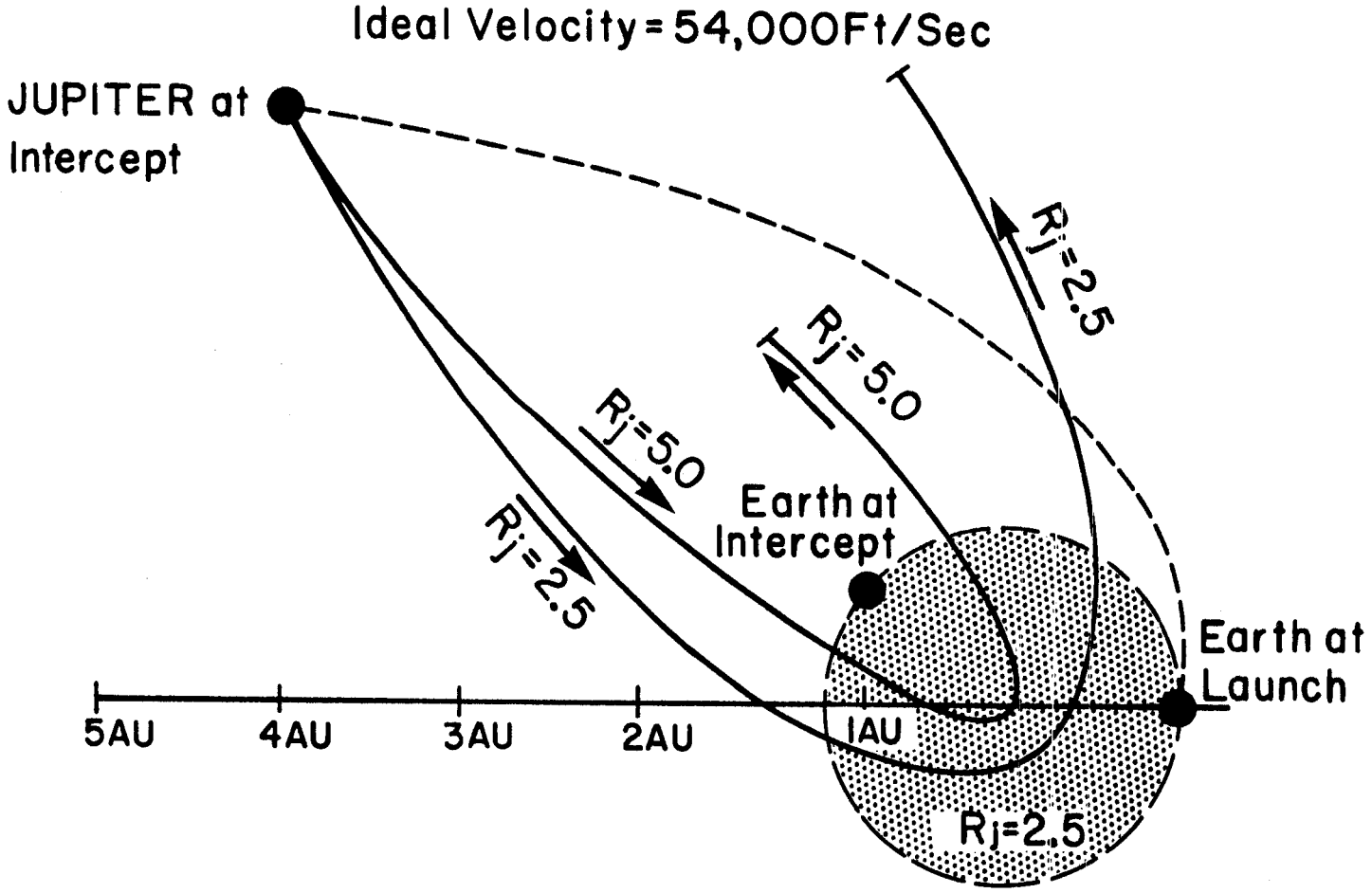

The 54,000 ft/sec, 500 day flight has the following desirable features, for both miss distances of 2.5 R_J and 5 R_J.

1. Jupiter is at opposition at intercept, so that communication distance at intercept is minimal (4.2 AU).
2. The spacecraft views both the light and the dark sides of the planet before it reaches minimum approach distance. Thus any possible damage to instruments by a proton radiation belt will tend to occur after most of the data have been obtained.
3. The spacecraft is injected into an orbit crossing Earth's orbit and passing near the Sun. Thus, stored information can be transmitted when communication distance is low, and the interplanetary regions near the Sun might be explored.

The energy, 54,000 ft/sec, and time of flight to Jupiter, 500 days, are not too severe requirements for modest payload missions in the early 1970s. For example, a 700-lb spacecraft, not including shroud and adapter, can be sent with an SLV3X-Centaur-Kick and a 1700 lb spacecraft can be sent with a Saturn 1B-Centaur.

2.3 Conclusions

1. A modest number of experiments carried out on a spacecraft fly-by mission to Jupiter can significantly add to present knowledge.
2. Most of the instruments capable of performing the critical measurements required are modifications of existing instruments that have been flown in spacecraft or of instruments currently in development under NASA sponsorship.

3. The distances of closest approach to Jupiter can be quite large up to 40 R_J, for significant yields from some of the most important experiments (No. 1, 5, 7, and 11 of Table 1).

4. Trajectory requirements for a particularly desirable mission are quite reasonable, requiring an ideal velocity of 54,000 ft/sec and a time of flight from Earth to Jupiter of 500 days.

3. DETAILED STUDIES OF JUPITER

3.1 Magnetosphere

The results from Mariner II and Mariner IV show that neither Venus nor Mars has an appreciable magnetic moment. In contrast, intense nonthermal radio emission indicates that Jupiter has a large enough magnetic moment to support an extensive magnetosphere.

Steady radio emission at decimeter wavelengths comes from a region roughly 6 R_J wide and 2 R_J high; this strongly implies the presence of large numbers of relativistic electrons trapped on lines of a magnetic field of considerable magnitude. Farther out, Io, a satellite of Jupiter, appears to trigger events that lead to intense bursts of radio emission at decameter wavelengths. These bursts can make Jupiter the brightest object in the sky over short times in a restricted frequency regime. How these bursts are triggered remains a

mystery, but their mere presence indicates interesting phenomena occurring inside Jupiter's magnetosphere.

Jupiter's field lines probably extend to about 50 R_J at the subsolar point and farther in other directions. A spacecraft missing the giant planet by as much as two million miles on the sunlit side and even farther on the dark side still intersects Jovian magnetic field lines.

Extensive reviews of the radiation from Jupiter can be found elsewhere (J. A. Roberts 1963, Smith and Carr 1963, Warwick 1964). The present review, while less complete in certain respects, is current and is oriented toward suggesting critical experiments that can increase present knowledge.

3.1.1 Decimeter Radiation

Analysis of the observed microwave (decimeter) radiation from Jupiter indicates the existence of a moderately large magnetic field and a belt of large numbers of relativistic electrons.

Since 1958 there have been an increasing number of observations of nonthermal radiation from Jupiter at and near decimeter wavelengths. A notable feature of these observations is the consistency of the results of various experiments. J. A. Roberts (1963) has summarized the individual observations.

The intensity of the total radiation, both linearly polarized and unpolarized components, is measured by radio telescopes of moderate resolution. They compare the radiation

flux from Jupiter with that from other radio sources. The flux of radiation received at Earth, normalized to an Earth-Jupiter distance of 4.2 AU, is given in Table 2. Most of the radiation was observed at wavelengths below 100 cm. Below about 10 cm the nonthermal radiation competes with fairly intense thermal radiation. Since it has been impossible so far to separate the thermal from the nonthermal component by any characteristic features in the radiation, the flux below 10 cm is not listed.

However, the frequency limits of the nonthermal radiation affect any estimate of the total output of radiation from Jupiter, since extrapolation of the intensity spectrum to small wavelengths indicates that approximately half of the radiation comes from wavelengths shorter than 10 cm. In computing the total output, we extrapolated down to 3 cm, with a cutoff at that point. This procedure is similar to that followed by Chang and Davis (1962).

A linearly polarized component is about 30 percent of the total radiation (Morris and Berge 1962). It is largest at the outer edges of the radiation region in the equatorial plane of Jupiter and at the longest wavelengths (31 cm) at which polarization is measured. The dependence of the amount of polarization on both wavelength and position is not great, however.

Attempts to measure a circular component of polarization from the radiation from Jupiter have been unsuccessful. The

Table 2

NONTHERMAL DECIMETER RADIATION CHARACTERISTICS

Quantity Measured	Value
Flux spectrum between 3 cm and 10 cm	Partly nonthermal
Flux spectrum between 10 cm and 100 cm	$(3\pm1) \times 10^{-26} (\lambda/\text{cm})^{0.3}$ watt/m^2/cps
Total nonthermal decimeter radiation	$(2.5\pm1) \times 10^9$ watt
Amount of polarization	$(30\pm10)\%$ linear $< 5\%$ circular
Angle between magnetic and rotation axes	9°
Rotation period	$9^h\ 55^m\ 29^s \pm 2^s$
Source size and location	3 R_J out in E-W direction 1 R_J out in N-S direction

percent circular polarization listed in Table 2 is an upper bound.

The plane of polarization as viewed from Earth oscillates with time. The amplitude of this oscillation is approximately ten percent on either side of the mean and can be accounted for by a constant angle between Jupiter's rotation axis and magnetic dipole moment of 9° (Morris and Berge 1962). The period of this oscillation of the plane of polarization is the same as the rotation period for emission of decameter radiation (within the errors of the experiment, Morrison 1962).

Since the disk of Jupiter is at the limit of resolution of most radio telescopes operating at wavelengths of the order of 20 cm, sophisticated techniques must be employed to resolve the radiation. Several methods have been used.

1. The most commonly used technique is interferometric. The results at 21 and 31 cm show that the radiation emanates from a region that is centered inside the disk of Jupiter and that extends to 3 R_J in an east-west direction and to 1 R_J in a north-south direction (Radhakrisknan and Roberts 1960).

   It is also possible to estimate the brightness temperature as a function of position by superimposing cuts across the region of Jupiter in both the north-south and east-west directions, but these brightness temperatures are subject to large errors. Results have been reported orally (Berge 1964).

2. Another method is an occultation method. In 1962 Jupiter was occulted by the moon in a roughly east-west direction to the radiation region. This occultation was observed in Australia by Kerr (1962), who reported that the total width of the radiation region at 70 cm was, as found before, 6 R_J.

Based on the fact that the source of the decimeter radiation from Jupiter extends well beyond the visible disk, the theories that might account for the observations are limited to cyclotron or synchrotron emission from radiation belts surrounding the planet. Both cyclotron and synchrotron emission are due to a single cause - the acceleration of charged particles (in this case, electrons) as they move in circles around a magnetic field line. Both types of emission lead to linearly polarized radio waves.

In cyclotron emission, the speed of the particle is small compared to the speed of light. Thus, an observer sees simple harmonic oscillation (SHO) of the charge at the cyclotron frequency (eB/mc).

In synchrotron emission, the particle moves at speed near the speed of light. The observer does not see SHO, because the time lag for the wave to get out of the particle's orbit is not small compared to the time the particle takes to move through its orbit. The wave is Doppler-shifted in various senses and by various amounts in each part of the particle's orbit. Thus the frequency of the wave coming out is not

"tuned" to the cyclotron frequency but is spread around the cyclotron frequency by a large factor.

Field (1959), who inaugurated a discussion of various theories, agrees with others that the decimeter observations, especially of the direction of polarization, cannot be explained by a cyclotron theory (1960, 1961).

Chang and Davis (1962) have computed what can be observed from a shell of relativistic electrons in a dipole magnetic field, with factors such as the magnitude of the magnetic field, the number and density of electrons, and the energy spectrum of these electrons left open as parameters. They concluded that the decimeter observations can be explained, even down to fine detail, by their synchrotron theory. Their explanation has now received widespread agreement. Unlike a cyclotron theory, synchrotron theory does not predict a unique magnetic field and number of electrons. It does, however, place constraints on these parameters.

Table 3 is a modification of a table by Chang and Davis (1962). It lists properties of the electrons in the radiation belts, assuming three different values of magnetic field strength at the radiation region, which is placed on field lines $L_J = 3$. The total radiation output in decimeter wavelengths from Jupiter acts as a fixed constraint on the product of the total number of radiating electrons and the magnetic field. If a further assumption, that the size of the radiation region is 10 times the volume of Jupiter, is made,

Table 3

PROPERTIES OF THE SYNCHROTRON RADIATION OF ELECTRONS IN A UNIFORM MAGNETIC FIELD

	Magnetic Field B (gauss)		
	0.1	1	10
Critical energy* E_c for radiation at wavelengths of (in mev):			
3 cm	75	25	7.5
30 cm	25	8	2.5
300 cm	8	2.5	0.8
Half-life of electrons (in years) at E_c	30	1	1/30
Gyroradius of electrons (in km) at E_c	10	1/3	10^{-2}
Number of electrons per cm^3 if total volume is 10 V_J+	2×10^{-2}	2.0×10^{-3}	2×10^{-4}
Electron energy per unit volume in erg/cm^3	8×10^{-7}	2.5×10^{-8}	8×10^{-10}
$B^2/8\pi$ in erg/cm^3	4×10^{-4}	0.04	4.0

* The critical energy, E_c (λ), for electrons which are to emit radiation of wavelength λ is 0.55 times the energy at which the power radiated per unit frequency interval has its maximum at λ.

\+ Number required to give the observed emission of Jupiter in the decimeter range.

the total radiation output yields the product of number density of electrons and the magnetic field.

The observed frequency spectrum of the radiation is used to determine the energy spectrum of the electrons making the radio emission. Since the nonthermal flux is only weakly dependent on wavelength (see Table 2), the electron energy spectrum in the radiation belts is also rather flat. It is interesting to note that a reasonably flat energy spectrum (a power law dependence with an exponent less than 2, for example) is similar to the extra-solar-system cosmic-ray spectrum. It may be that energetic long-lived charged particles undergoing some form of magnetic acceleration may commonly have rather flat energy spectra, a suggestion originally made by Fermi (1949).

The fact that the emission is synchrotron, which requires relativistic electrons, places an upper bound to the size of the magnetic field in the radiating region. The critical energy shown in Table 3 must be significantly greater than the rest energy of an electron if the electrons are relativistic. The longest wavelength at which it is certain that a cyclotron theory breaks down is about 30 cm, and so the critical energy at 30 cm must be significantly greater than the rest energy of an electron, i.e., at least 1 mev. A calculation shows that this places an upper bound to the magnetic field at the radiating region of about 75 gauss.

3.1.2 Decameter Radiation

Observations of decameter radiation coming from the direction of Jupiter were made in 1955, somewhat earlier than the first decimeter observations. Rather than existing as a steady radiation, it is emitted in short bursts that last from less than one second to hours. The radiation is sharply tuned in frequency, having bandwidths of the order of 1 Mc. It occurs most strongly at center frequencies of the order of 20 Mc, with no emission above 42 Mc. The center frequency of each burst drifts in time, some toward higher frequencies and some toward lower.

A basic parameter describing a burst is whether it is of sufficient intensity to be detected by a given, tuned receiver at a given time. It has been found that the probability of emission recurs in a periodic fashion with a period similar to but not identical with the planet's rotation period in System II.*

Features in the observed decameter radiation also show a periodicity, indicating rotation at $9^h55^m29.5^s \pm 1^s$. System III was invented to display decameter radiation features, such as probability of emission, as a function of the longitude of Jupiter facing Earth, where the features are nearly stationary

---

* The only visible features one can observe on Jupiter lie in its atmosphere. Almost all non-equatorial belt features rotate with nearly the same speed, about $9^h55^m41^s \pm 20^s$, the fluctuations caused by variable winds. System II is a coordinate system which rotates with a speed matching a suitable average rotation of non-equatorial belt features (period $9^h55^m41.632^s$). Non-equatorial features then appear at nearly fixed longitudes in the System II system.

in time. Its period is defined to be $9^h55^m29.37^s$.

A typical display of new data is shown in Figure 3, which is taken from Smith et al. (1965). The radiation is most intense at frequencies of 22 Mc and 18 Mc with significantly less radiation at the higher frequency and a slow trailing off toward the lower frequency. Because effects of the Earth's ionosphere become important at frequencies below 10 Mc, the trailing off there may not be real. This relatively narrow frequency spectrum differs greatly from the almost flat decimeter spectra.

The probability of emission at the higher frequencies is thus a function of the Jupiter longitude facing Earth and is at a maximum when the Jupiter longitude is approximately 130°, 240°, and 300°. These peaks have been called sources B, A, and C by some experimenters. Warwick and coworkers call the B peak the early source and the A and C peaks the main source, on the basis of swept frequency analysis of the spectral character of the bursts.

The probability distributions can also be converted to power distributions, as shown in Figure 4. Again, there is a marked dependency on System III longitude. From these curves and others, the total average flux energy at Earth can be estimated. This can be used to compute the total power emitted from Jupiter, assuming that Jupiter radiates in all directions with an equal total probability on the average. The result of

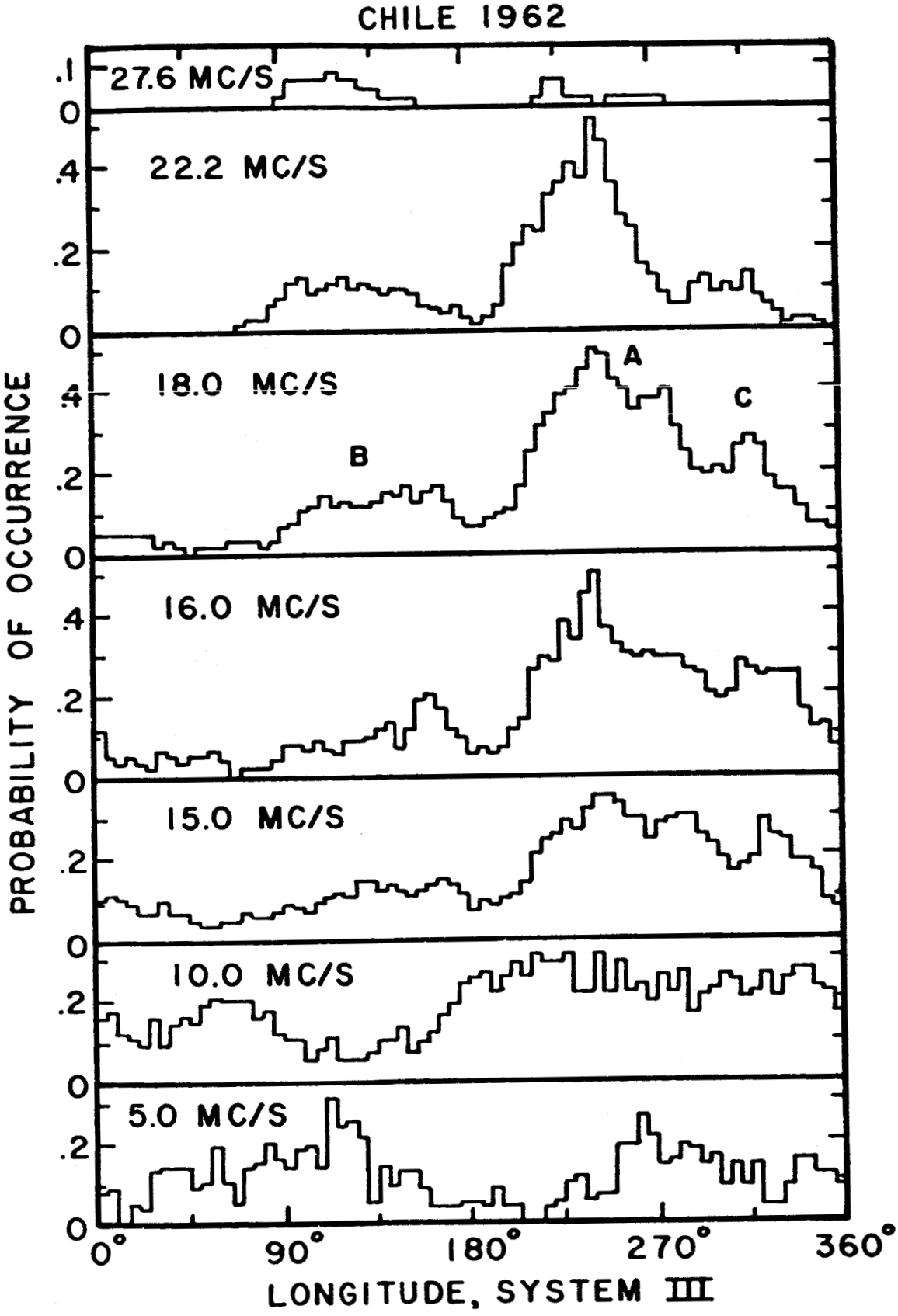

Figure 3 HISTOGRAMS OF PROBABILITY VERSUS SYSTEM III (1957.0) LONGITUDE FOR THE 1962 OBSERVATIONS MADE IN CHILE

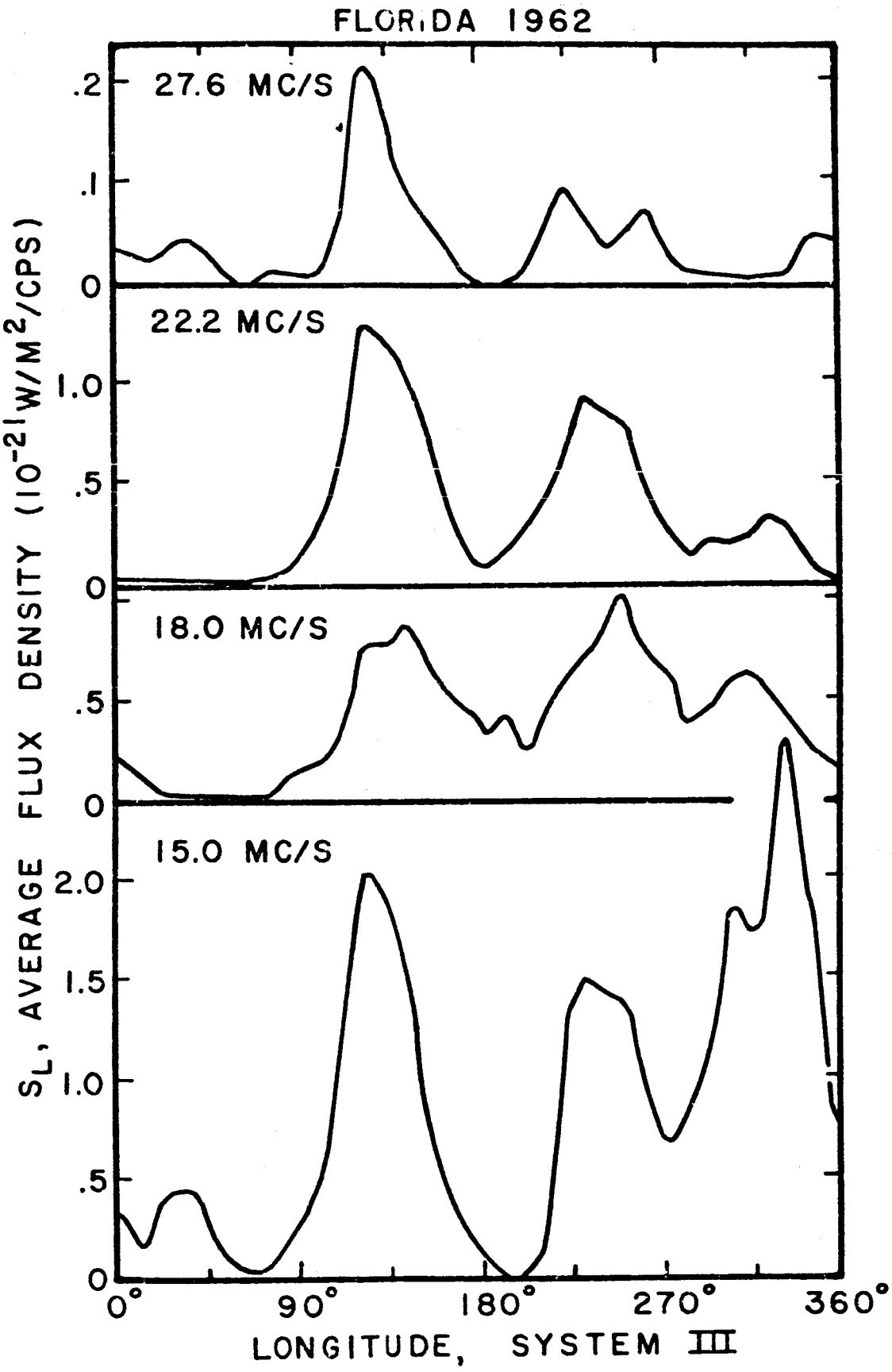

Figure 4 PROFILES OF THE AVERAGE RECEIVED FLUX DENSITY S_L VERSUS SYSTEM III (1957.0) LONGITUDE FOR THE 1962 FLORIDA OBSERVATIONS. THE AVERAGE IN THIS FIGURE IS TAKEN OVER ALL EFFECTIVE LISTENING TIME. THREE-POINT SMOOTHING HAS BEEN EMPLOYED. NOTE THAT THE VERTICAL SCALE HAS BEEN EXPANDED FOR 27.6 MC/S

this calculation is that the total radiated power in decimeter wavelengths is only slightly less than the total power at decimeter wavelengths (Table 2); that is, the total radiated power from Jupiter in decameter wavelengths is $\sim 10^9$ watts.

A recent and noteworthy discovery made by Bigg (1964) is that the emission probability is a function not only of the longitude but also of the position of the innermost Galilean satellite of Jupiter with respect to the Earth-Jupiter line. This means that plotting the probability of emission versus Jupiter longitude gives an incomplete description.

In a recent report, Warwick and Dulk (1965) summarize the most recent observations (January 1964-May 1965). Figure 5, which is taken from their report, shows the dependence of the probability of emission on both the position of Io in orbit and the Jupiter longitude. The presentation is in the form of a contour map, each contour representing a given probability of emission. Note that the early source "emits" with significant probability only when Io's position is about 90° from superior conjunction. (Superior conjunction occurs when Io is on the Earth-Jupiter line, behind Jupiter.) Furthermore, the main sources emit with greatest probability when Io's position is near 240° from superior conjunction, with a lesser peak at 90°. Thus, to a first approximation, the probability of emission is significant only when both Jupiter's longitude and Io's position are at one of the favored sets of locations: (90°, 140°), (240°, 200°-340°) and (90°, 240°).

Dulk (1964) has analyzed the spectral content of the early source emission, i.e., the (90°, 140°) region. He found

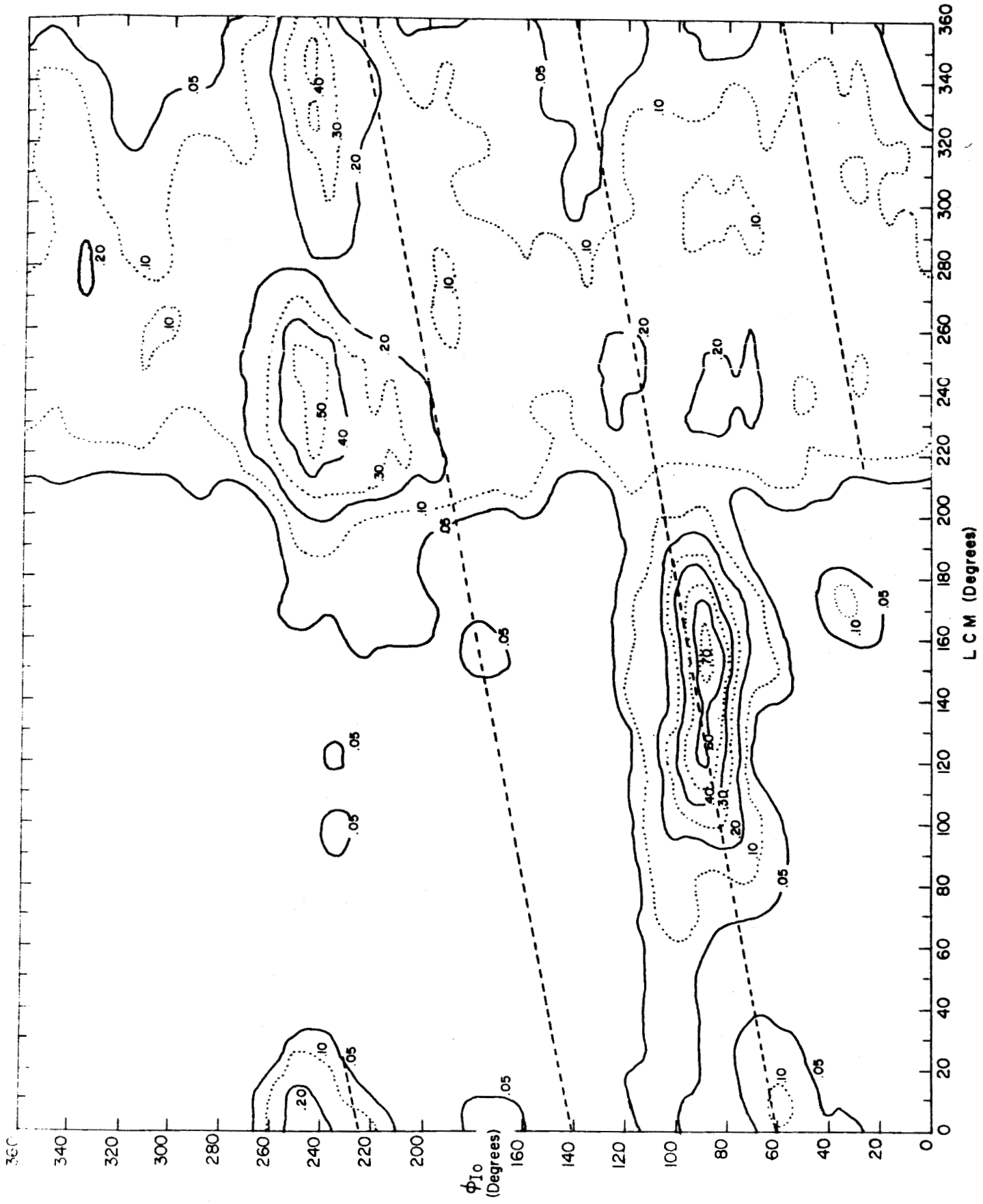

Figure 5 Estimated joint probability distribution for emission as a function of the LCM and the Io position. Emission probability is labeled on the contour lines. The diagonal dashed lines illustrate the path of the LCM - Io phase point, through one day, starting at 0^h UT on 1 Jan 65.

that the spectral character of a burst, i.e., intensity against frequency as a function of time through a burst, is nearly the same for all bursts at early source conditions and is very different from the early source character for all other bursts. Thus, Io, which lies at 6 R_J, has a profound influence on the radio emission from Jupiter.

Another feature of note in the decameter bursts is that the radiation is elliptically polarized, with a preponderance of right-hand circular polarization over left-hand from the Jupiter longitudes where emission is observed.

Douglass has reported a lengthening of rotation period of the sources in the last few years. Figure 6, which is reproduced from Smith et al. (1965), indicates this drift in longitude of the red spot. Dulk and Gordon (1965) report a recent decreasing drift, similar to the decreasing drift shown for the red spot. This correlation in changes of rotation rates may be attributable to a common cause and may indicate strong magnetic influences on the red spot.

The observations over the last few years indicate a definite correlation with solar activity. Figure 7, also taken from Smith et al. (1965), displays this correlation. A minimum of decameter burst activity occurs one year after sun-spot minimum, a behavior remarkably similar to cosmic-ray activity.

The results of the decameter observations are summarized in Table 4. The very complexity of this radiation indicates

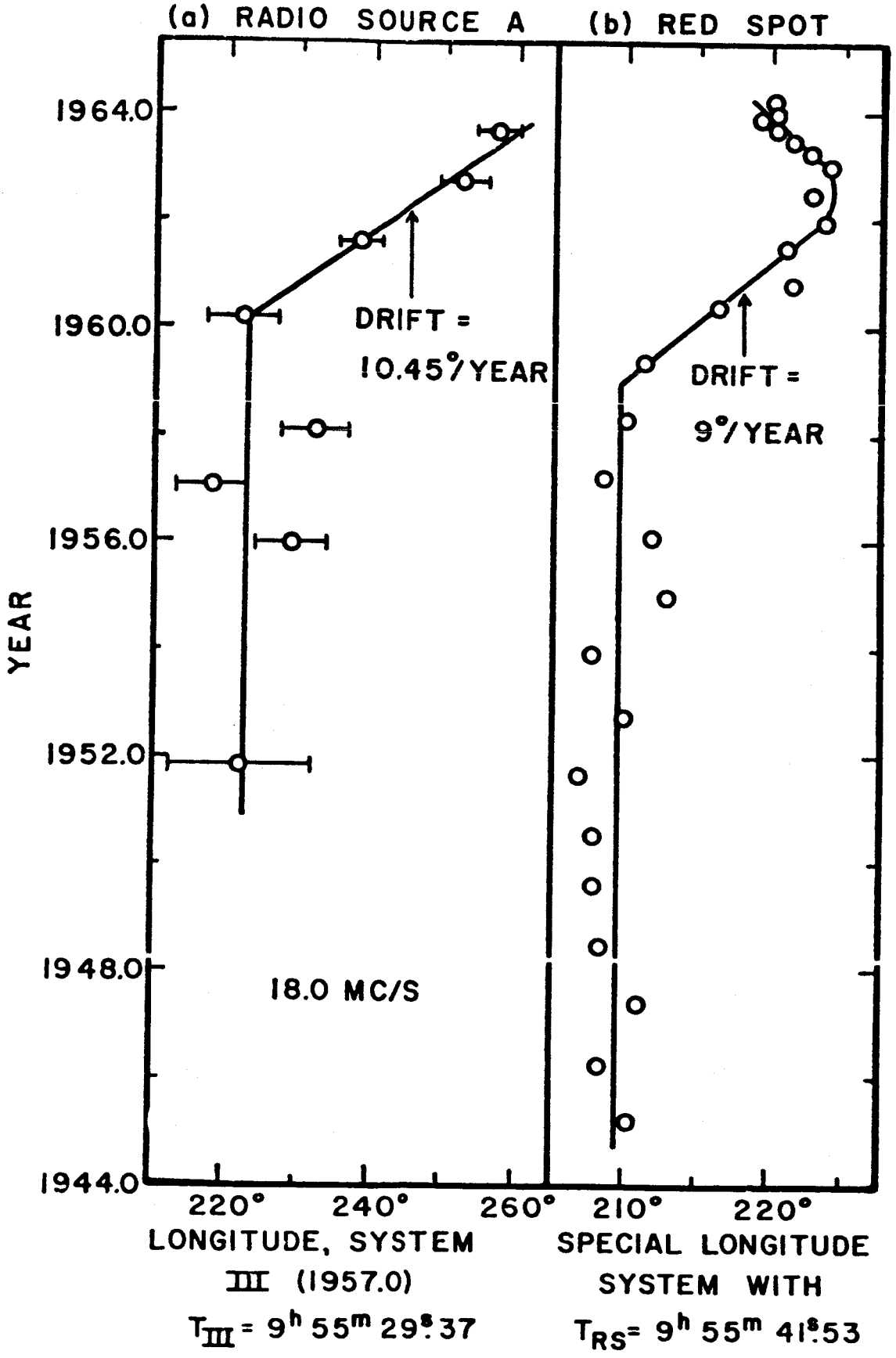

Figure 6 (a) DRIFT OF SOURCE A IN SYSTEM III (1957.0) COORDINATES; (b) DRIFT OF THE GREAT RED SPOT IN A SPECIAL LONGITUDE SYSTEM DESIGNED TO MINIMIZE ITS MOTION FROM 1945 TO 1959.

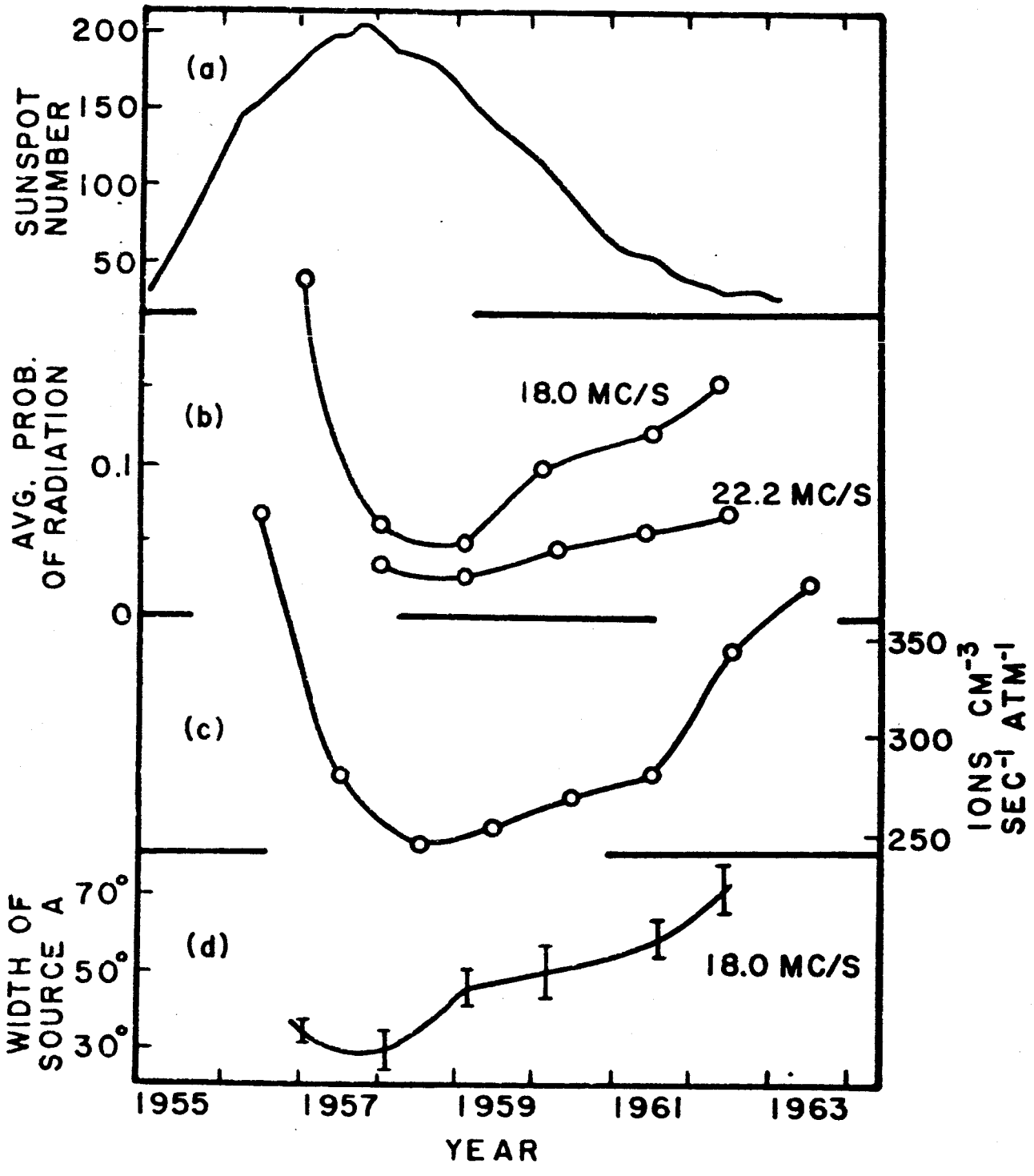

Figure 7 LONG-TERM VARIATIONS OF (a) MONTHLY AVERAGES OF THE ZURICH SUNSPOT NUMBER: (b) APPARITIONAL AVERAGES OF JOVIAN RADIO-FREQUENCY ACTIVITY; (c) IONIZATION CREATED BY COSMIC RAYS NEAR THE TOP OF THE EARTH'S ATMOSPHERE (AFTER NEHER AND ANDERSON 1964); (d) WIDTH IN DEGREES OF LONGITUDE OF JOVIAN SOURCE A, MEASURED AT THE HALF-AMPLITUDE LEVEL OF THE 18-MC/S PROBABILITY HISTOGRAM FOR EACH APPARITION.

Table 4

DECAMETER RADIATION CHARACTERISTICS

Flux:

Highly variable

Estimated total decameter radiation:

2.5×10^9 watts; 5 Mc $< f <$ 40 Mc

Rotation period:

$9^h\ 55^m\ 29^s \pm 1^s$ Years: 1952-1960

Change of rotation period:

Similar to red spot's change Years: 1960-1963

Correlation with solar activity:

Similar to that of cosmic rays Years: 1958-1962

Probability conditions of emission maximum:

Position of Io	Jupiter Longitude
90°	140°
240°	200°-340°
90°	250°

Frequency bandwidth per burst:

$\sim$1 Mc

Frequencies of emission:

5 Mc to 40 Mc

Polarization:

Right-hand circular for 90% of bursts $f > 18$ Mc

Less right-hand polarization than 90% $f < 18$ Mc

that, if it were understood, it would yield a great deal of data on Jupiter's magnetosphere. A complete theory explaining all the facts uniquely has not been proposed, although several theoretical deductions have been made. Two possible theories, both incomplete, have been proposed to explain these observations.

Ellis and co-workers in Australia (Ellis 1962, Dowden 1962, Ellis 1963a, b) have proposed that the radiation is generated by cyclotron emission from electrons in a radiation belt. Warwick (1961, 1963a, b) on the other hand, has proposed that the radiation is generated by Cherenkov emission from electrons being dumped along field lines in polar regions, the radiation reflecting off the surface of the planet or its ionosphere and being beamed to Earth. (Cherenkov radiation is the electromagnetic radiation present when the speed of a moving disturbance exceeds the phase velocity of waves in the surrounding medium.)

The theories are not mutually contradictory, so it is possible that both or neither proposed mechanism contributes to the radiation. Both Ellis and Warwick start with a magnetosphere much like Earth's except that the number of energetic electrons is assumed to exceed Earth's by a factor of 100 to 1000. The field and the particle configuration required for the theories are summarized in Table 5.

Of the two theories, Warwick's more completely describes the magnetic field and energetic electron distributions near

Table 5

DECAMETER RADIATION THEORIES

	Ellis:	Warwick:
Electron energy:	10-100 kev (assumed)	10 kev (assumed)
Magnetic field :	8G at L = 1, equator (assumed)	10G at L = 1, equator (concluded)
Number density :	$\frac{eB}{m_e c} / \frac{4\pi ne^2}{m_e}$ (required) (n at L = 6 = 250-4000/cm^3)	10^3 x n_{Earth} at 10 kev (assumed) (n at L = 6 = 10^4-10^5/cm^3, if low energy electrons also have 10^2-10^3 n_{Earth}).
Comment :	This theory explains the polarization data, but requires significant departures from a dipole field at the ratiating region in order to explain the Jupiter longitude source distribution.	This theory explains the very complicated spectral characteristics of the bursts and the longitude dependence, but the magnetic field configuration arrived at may be in contradiction to some decimeter observations recently reported by Berge and Morris (1964).

Jupiter. The physical mechanism for the radio emission is as follows. Electrons, which somehow have been scattered in pitch angle (by Io?) such that they are no longer trapped in Jupiter's magnetosphere, stream down a field line toward Jupiter's ionosphere or surface and eventually encounter a magnetic field strength sufficiently high that their speed exceeds the speed of the extraordinary wave in the medium. Some kinetic energy is then converted into Cherenkov radiation, which goes preferentially in the forward direction, i.e., toward the planet. This radio emission is reflected by either the ionosphere or the surface of the planet.

The geometry of the reflections is used to calculate a longitude profile and a frequency drift spectrum. The method is as follows. Jupiter is assumed to have a dipole magnetic moment of unknown strength and position originating inside its core, which is tilted at 9° from the rotation axis, as required by the results of the decimeter radiation. The field lines are chosen such that an equatorial electron starts its journey down the field line at a distance of 3 R_J. (This choice was made before it was known that Io is important; now it would be better to consider particles starting at L = 6, although the results are apt to differ by about a factor of only 2 or less.) Then it is possible to fit the frequency spectrum-time profiles very well if it is assumed that the magnetic field is an off-centered dipole on the Earth-Jupiter line when the Jupiter longitude facing Earth is 200°, located as shown in Figure 8. The size

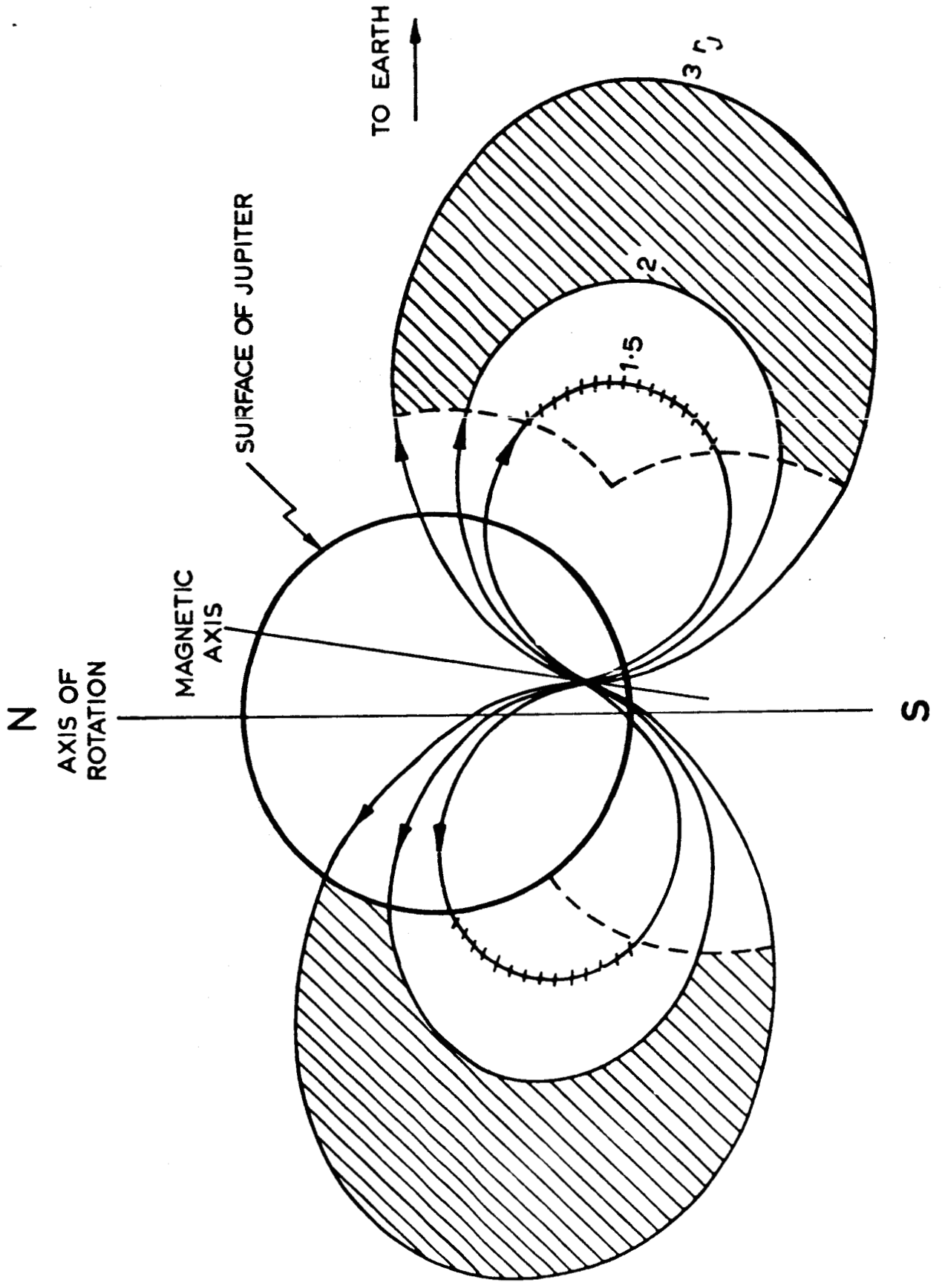

Figure 8 THE CONFIGURATION OF THE JOVIAN MAGNETIC DIPOLE FIELD AND THE RADIATION BELTS ACCORDING TO THE THEORY OF WARWICK. THE SECTION SHOWN IS AT $\lambda_{III} = 200°$. THE DOTTED CURVES SHOW THE LIMITS TO THE RADIATION BELTS IMPOSED BY COLLISION WITH THE PLANET.

of the magnetic dipole moment is determined by the frequency scale and gives a field of 0.43 gauss at the equator of the field line at L = 3.

This theory fits the following observations: the elliptical polarization, the frequency spectrum-time profile, and the longitude profile. The radiation is predominantly right-hand polarized, which permits determination of the direction of the magnetic field.

3.1.3 Magnetic Field and Radiation Belts

The results of the observations and theories about the radio radiation from Jupiter can be used to estimate the properties of Jupiter's magnetic field and radiation belts. Table 6 compares the properties of Jupiter's and Earth's magnetospheres. The reliability of the values given varies. Those values that come most directly and unambiguously from the observations, such as the dipole axis-rotation axis angle, are quite reliable; whereas those that come from a tentative theory such as the dipole position, are much less reliable. The numbers in the right-hand column of Table 6 give an estimate of the relative reliability of the values, 10 being the most reliable and 1 the least reliable.

The size of the magnetic field is deduced by using Warwick's theory. A factor increasing the reliability of the value is that the magnetic field size at L = 1 implies a field of about one gauss in the relativistic electron radiation belt, and

Table 6

DEDUCED FIELD AND PARTICLES

	Earth	Jupiter	Relative Reliability of Jupiter Values
A. Magnetic Field			
1. Field strength at magnetic equator	.31 gauss	10G $\begin{cases}+10G \\ -5G\end{cases}$	5
2. Field dipole (to 1st approximation)?	Yes	Yes	7
3. Angle between dipole axis and rotation axis	11.4°	9° ± 2°	10
4. Position of dipole center	20° off center	As in Figure 8	2
		> 20° off center	9
5. Size of magnetosphere (sunlit side)	10 Earth radii	50 ± 10 R_J	8
B. Electrons			
1. Density of ~1 mev electrons at L=2-3	$\sim 10^{-6}/cm^3$	$n_e \sim 10^{-2}/cm^3$	4
2. Energy spectrum of ~1 mev electrons at L=2-3 (power law spectrum: $N(E)dE \propto E^{\gamma}dE$	None known	$\gamma = -1 \pm 1$	6
3. Density of electrons between 10 kev and 100 kev at L~6, magnetic equator	$\sim 1/cm^3$	$n \sim 10^3/cm^3$	3
C. Protons			
1. Density of ~10 mev protons at L~1.5-3	$\sim 10^{-4}/cm^3$	$n \sim 10^{-1}/cm^3$	1

Note: For purposes of this table, "~" means one order of magnitude, centered on the value following the "~". "10" is the most reliable value; "1" is the least reliable.

one gauss lies in the middle of the range suggested by Chang and Davis (Table 3).

The orientation of Jupiter's magnetic field is deduced from the oscillation of the plane of polarization of the decimeter radiation and is quite reliable. The position of Jupiter's dipole center, on the other hand, is the feature most open to doubt, because it is deduced from a controversial theory. If the magnetic field is really as far off center as is shown in Figure 8, the field strength at the point on Jupiter's surface nearest the dipole can be as much as 500 times the field strength at the surface at the farthest point.

Finally, it is possible to compute the size of Jupiter's magnetosphere. We assume that the solar wind flux declines with distance according to an inverse square law, and we set the magnetic pressure of a compressed dipole Jupiter field at the edge of the magnetosphere equal to the solar wind pressure there. The result is a 50 R_J magnetospheric size at the sub-solar point. The reason for the relatively high reliability shown in Table 6 is that large differences in Jupiter's magnetic moment lead to only small changes in magnetospheric size.

Properties of the radiation belts' radiation are also listed in Table 6. The results from decimeter radiation, such as the relativistic electron density and energy spectrum, are more reliable than the results from decameter radiation. Even if Warwick's theory is correct, the electron conditions are not uniquely specified at L = 6.

Protons, because of their much greater inertia, do not leave a radio emission "signature" as do electrons. We can tentatively postulate that protons exist by considering the magnetosphere of Jupiter as a whole. The evidence indicates that there are about 10^3 times as many relativistic electrons in the inner-electron zone of Jupiter than there are on Earth. Furthermore, Warwick's postulate that the outer electron zone near L = 6 contains about 10^3 times more $\sim$10 kev electrons than Earth fits the observations. Therefore, the extrapolation that the number of hot protons in Jupiter's magnetosphere is also about 10^3 more than on Earth is made, though with low reliability. This extrapolation implies that Jupiter has an inner Van Allen belt composed of the numbers of hot protons shown in Table 6, and such a belt might cause an intense radiation hazard to a passing vehicle.

3.1.4 Spacecraft Measurements

At present, the configuration and the magnitude of the magnetic field are not well known. Of the many mechanisms proposed for emission of decameter bursts, none is completely satisfactory. The ambiguities about the fluxes, magnetic field strength, and energy spectra of the relativistic electron belt have not been solved, despite the extensive observations of decimeter radiation. Energetic fluxes have only been postulated, without any supporting experimental evidence except by analogy to Earth.

In order to increase our knowledge of Jupiter's magnetosphere by a spacecraft fly-by mission, we recommend a "particles and fields" experimental package similar to that carried on the IMP satellites. Table 7 lists the relevant experiments. These crucial experiments would make four important measurements of the environment: the magnetic field; moderate-energy electrons as expected near L = 6; high-energy electrons as expected in the innermost radiation belt, where L = 2 to 3; and high-energy protons.

The amount of useful information depends on the proximity of the spacecraft to Jupiter. Miss distances of 25 R_J, 5 R_J and 2.5 R_J are approximate maximum miss distances at which a new "level of information" can be obtained because the spacecraft then spends considerable time within 40 R_J, 6 R_J and 3 R_J respectively.

A spacecraft that comes within 2.5 R_J spends approximately 2 hours at distances < 3 R_J. Therefore, it can obtain "complete" information concerning Jupiter's magnetosphere. The magnetic field configuration and the size can be determined. Measurements of moderate-energy electrons near L = 6 might provide a key to understanding the decameter bursts. This information can then be used to understand time-dependent processes. Measurements of the flux of relativistic electrons are of intrinsic interest, and, when coupled with the magnetic field measurements, can check the synchrotron theory of

Table 7

RECOMMENDED EXPERIMENTS

Instrument	Measured Quantity	Range
1. Magnetometers	Magnetic field	5×10^{-6}-10 gauss*
2. Moderate energy electron counter	Flux of electrons in steps from 10 kev to 1 mev	10^{9}-10^{13}/cm^{2}sec kev
3. High energy electron counter	Flux of electrons in steps from .8 mev to 100 mev	10^{4}-10^{6}/cm^{2}sec mev
4. Proton counter	Flux of protons above 30 mev	10^{8}-10^{11}/cm^2 sec

* The upper limit of the range, 10 gauss, assumes that the distance of closest approach will be 2.5 R_J. Upper limits for missions having larger miss distances are not as large, e.g., upper limits are 1 gauss for 5 R_J and 5×10^{-3} gauss for 25 R_J.

decimeter emission and remove the ambiguities. Possible proton radiation belts might be found by direct measurements.

A spacecraft that goes as far in as 5 R_J can obtain almost complete information. Again, the size and the configuration of Jupiter's magnetic field can be measured, as can the electrons near L = 6. Knowledge of the magnetic field of Jupiter can be used to estimate the number density of electrons in the inner radiation belt by employing the relations shown in Table 3, though with less certitude than a mission within L = 3.

Finally, some very useful information can be obtained if the spacecraft barely penetrates Jupiter's magnetosphere. Knowledge of the size of Jupiter's magnetosphere anywhere within that magnetosphere can determine the size of the magnetic moment to within a factor of two; this is based on observations made by IMP I. On the basis of present knowledge, the boundary between Jupiter's magnetosphere and the outside lies at about 50 R_J out on the sunward side and even farther out in other directions. Even with a miss distance of 25 R_J, the spacecraft is almost certain to be inside Jupiter's magnetosphere for several hours. A miss distance of less than 25 R_J is relatively easy. The target presented by Jupiter's magnetosphere to an observer on Earth is a circle of radius 25 R_J, or of diameter (1/2)° of arc. This implies a target cross section whose angular dimensions are the same as the moon - a large target indeed, by comparison to other planetary targets.

To summarize, it is clear that our understanding of the radiation belts and magnetic field of Jupiter can be increased enormously from a mission to Jupiter that misses by as large a distance as 25 Jupiter radii, and, of course, the amount of information obtained increases with closer approaches.

3.2 Atmospheric Composition

3.2.1 Major Constituents

Absorption bands attributed to the atmosphere of the planet were detected in the spectrum of Jupiter in the last century. They were unidentified for over fifty years, however, until Wildt (1932) showed that methane (CH_4) and ammonia (NH_3) were the absorbing gases. Abundances of 150 and 7 meter atm,* respectively, were subsequently derived by Kuiper (1952).

These remained the only two positively identified constituents for almost thirty years, but converging theoretical and experimental evidence strongly supported the presence of large amounts of hydrogen and/or helium. The theoretical evidence came from speculations about the origin of the solar system based on the observed abundances of the elements in the Sun and stars. Hydrogen is the main constituent of the observable universe, and helium is next. Furthermore, Jupiter has a low mean density (ρ = 1.33), which suggested a radically different composition from that of the Earth (ρ = 5.52).

* One meter atmosphere is the thickness of a layer of gas when reduced to standard temperature and pressure. It is equivalent to 2.69×10^{21} molecules/cm^2.

The first experimental verification of this line of reasoning resulted from an observation made by Baum and Code (1953) of an occultation of a star by Jupiter. As a planet moves in front of a star, the starlight passing through the planet's upper atmosphere is spread out by refraction. As a result, the light from the star begins to fade at a rate that depends on the rate of increase of atmospheric density with decreasing height above the surface of the planet. By observing this fading of the starlight, it is possible to derive a value for the scale height of the atmosphere at the mean level at which the occultation takes place. The scale height is $H = \frac{RT}{mg}$, where R is the universal gas constant, T the mean atmospheric temperature, m the mean molecular weight, and g the acceleration of gravity. Assuming a value of T = 86°K based on a model of the atmosphere derived by Kuiper (1952), Baum and Code determined a value of $m = 3.4 \pm 2.0$. Such a low value of the molecular weight obviously excluded an atmosphere predominantly composed of methane (m = 16) or ammonia (m = 17) and strongly suggested the presence of substantial quantities of the two lightest, cosmically most abundant gases.

Measurements of the abundance of hydrogen in the Jovian atmosphere are different. Because the hydrogen molecule is homonuclear (to a first approximation, nuclei in the molecule are identical), its interaction with sunlight is extremely weak, leading to extremely faint absorption spectra. Direct proof of the existence of hydrogen in the atmosphere was obtained

by Kiess, Corliss, and Kiess (1960), who observed four lines of a molecular band near λ8150 Å.

The first attempt to derive a hydrogen abundance was made by Zabriskie (1962), who obtained a value of 3.5 km atm by using the spectra of Kiess et al. A subsequent determination by Spinrad and Trafton (1963), based on their own spectra, led to a value of 27 km atm. They also reported the detection of an even weaker hydrogen absorption line at λ6367.80 Å, although their abundance determination, like Zabriskie's was based on the λ8150 Å lines. Foltz and Rank (1963) showed that the mere presence of the λ6367.80 Å line indicated that the Jovian atmosphere must contain immense amounts of hydrogen, perhaps an order of magnitude more than that reported by Spinrad and Trafton. The lack of agreement in these values is due to the difficulty in measuring the exceedingly narrow lines. Also, saturation could exist and escape detection.

Using the data of Foltz and Rank plus the methane abundance derived by Kuiper, and assuming that the C/H ratio was the same in the atmospheres of Jupiter and the Sun, Owen (1965) suggested an abundance of 190 km atm. Using a value for the equivalent width of the λ6367.80 Å line reported by Spinrad and Trafton (1963), Field (1963) concludes that the amount of hydrogen in the atmosphere of Jupiter lies between 30 and 80 km atm, with some preference for the

lower values. His adopted value is based on the revision of Foltz and Rank's work (1963) by Rank, Fink, Foltz, and Wiggins (1964) and takes into account the possibility that the lines are somewhat narrowed rather than broadened by pressure. Now that a more accurate value for the absorption coefficient is available, the precision of the abundance determination can be improved by additional measurements of the equivalent widths of the quadrupole lines. In any case, it is evident that with respect to hydrogen, methane and ammonia are minor constituents.

The problem of a determination of the abundance of helium is more difficult. The ground-state lines of this atom lie far out in the ultraviolet, well below the wavelength at which the Sun ceases to appear as a continuous radiator. Thus, even when it is possible to observe the planet from above the Earth's atmosphere (which cuts off radiation below 3000 Å), it is unlikely that helium will be detected in this way. There are two other approaches that may prove useful, however.

One is an investigation of the pressure broadening of methane and ammonia lines. If it is possible to interpret the observed line profiles in terms of a mean atmospheric pressure, enough helium can be added to the known amounts of methane, ammonia, and hydrogen to produce the required pressure. This approach must include a consideration of the possible presence of relatively large amounts of neon, whose ground-state absorptions are also likely to be undetectable. The mean

molecular weight provided by the scale height determination of Baum and Code (1953) would serve as a check on the neon abundance.

The second method for detecting helium would also be suitable for neon. This consists of a search for upper-state transitions that would produce emission lines. These features would be expected to occur in the upper atmosphere of the planet, in analogy with the terrestrial aurora and airglow. They could be detected by a suitably instrumented spacecraft passing behind Jupiter (as seen from the Earth) and permitting observations of the unilluminated hemisphere (the "night sky").

3.2.2 Trace Constituents and Atmospheric Photochemistry

The abundances of the atmospheric constituents discussed in the preceding section have been deduced either from direct observation or by simple analogy with observed cosmic abundances. The question of the possible existence of trace constituents (gases present in amounts comparable to or smaller than the observed abundances of ammonia and methane) requires a more sophisticated approach. There are two principal arguments for postulating the presence of small quantities of polyatomic gases other than those observed directly. One is purely theoretical, based on likely photochemical reactions which should occur in a Jovian-type atmosphere. The second is the evidence presented by the colors observed in the visible cloud layers. The implications of these arguments and their interrelation will be considered in this section. The photochemistry

of ammonia and methane is discussed in some detail since these gases are the most important sources of more complex substances.

The photochemistry of any atmosphere containing more than one constituent is a complex matter.

Cadle (1962) was the first person to attempt calculations on the kinetics of the photochemical reactions in Jupiter's atmosphere. He uses the abundances shown in Table 8.

Table 8

COMPOSITION ESTIMATES
(from Cadle 1962)

Hydrogen	6.8×10^5 meter atm
Helium	1.9×10^5
Neon	6.3×10^2
Methane	1.5×10^2
Argon	8.5×10
Ammonia	7.0

These figures all refer to the atmosphere above the cloud surface only. The figures for ammonia and methane were obtained from Kuiper (1952), and the remainder were obtained from Kuiper's calculations on the composition of the initial gaseous envelope. Opik (1962) gives different values, in particular, 97.2% of helium and 2.3% of hydrogen.

The possible presence of water is not excluded on chemical grounds but is excluded on thermal grounds (above the cloud layer). Water would be completely condensed out at the prevailing low temperatures. Carbon dioxide would be completely

reduced to water and methane. Opik (1962) states that free nitrogen would not exist in such an atmosphere.

Cadle rightly refers to his calculations as a simplified model. He ignores many reactions that are known to occur in photolysis. It is difficult to understand why he omitted all reactions involving the NH molecule, because it is known to be created by the ultraviolet irradiation of $\bar{N}H_3$. Quite a few of the other possible reactions have also not been treated. Cadle includes only exothermic or very slightly endothermic reactions. This is because appreciable thermal excitation is not to be expected at the low prevailing temperatures. However, many reactions which he omitted are in fact of this type.

Cadle considers three different levels in the atmosphere, defined by the fraction of radiation absorbed down to the levels concerned, (e.g., Lyman-α for methane). His results show zero ammonia concentration at these levels. The lowest level was that at which 50 percent of the radiation most strongly absorbed by ammonia remained. Cadle did not include all the NH_3 regeneration cycles which can be proposed, in fact he only used one:

$$NH_2 + H + M \longrightarrow NH_3 + M \qquad (1)$$

He might also have considered the possibility

$$NH_3 + H \longrightarrow NH_4 \qquad (2)$$

$$NH_4 + NH_2 \rightleftharpoons \begin{matrix} 2NH_3 \\ NH_3 + H_2 + NH \end{matrix} \qquad (3)$$

as these reactions should be exothermic.

Cadle's results gave zero ammonia concentrations at all levels, which is in disagreement with the measured 7×10^5 m atm abundance. He suggested that this disagreeement with observation be due to inadequate allowance for H_2 absorption. The omission of some of the other reactions could also be a major factor.

The variety of colors observed in Jupiter's atmosphere is associated with the chemistry of the atmosphere. These colors, observed in the cloud belts, range over blue, green, yellow, brown, and red in various shades. The great red spot is the most familiar of these and has received special attention. These colors change with time. They may have a stability of weeks or months or less. The patches in which they occur do not necessarily rotate at the planet's rotational velocity; this indicates fluid motion of some sort. Peek (1958) points out that the colors on Jupiter are distinct but the contrasts are not as strong as the average description leads one to believe. Peek refers to these colors as usually consisting of yellow zones and grey belts.

Urey and Brewer (1957) suggest that fluorescence from ions and radicals produces these colors. They point out that such ions and radicals as NH_2, N_2^+, CN, CH^+, CH, and C_2 can all be formed by the absorption of radiation by NH_3 and CH_4 and that these molecules all radiate in the visible at various wavelengths:

Red	NH_2, C_2, CH_2
Blue	NH, H_2^+, CN, CH, CH^+

Urey (1959) also points out that many C-H-N compounds are highly colored:

Diazomethane	CH_2N_2	yellow
Tetrazine	$C_2H_2N_4$	red
Azomethane	$(CH_3)_2N_2$	yellow
Cuprene	$(C_2H_2)_n$	yellow

If aromatic compounds (i.e., those containing a benzene ring) are included, many more colored substances are possible.

Rice (1956), too, explains the colors on the basis of formation of radicals. He observed solid NH in the laboratory upon the thermal decomposition of hydrazoic acid (N_3H). The NH was stable at liquid nitrogen temperatures, forming a blue solid. On being warmed, it suddenly turned white at -125°, becoming ammonium azide (NH_4N_3). In another experiment he collected a yellow solid, presumably NH_2NH, from the thermal decomposition of hydrazine (N_2H_4). On warming, it turned white at -178°, giving off nitrogen. On Jupiter the free radicals would be formed in the high layers of the atmosphere and swept down to the colder regions, where they would condense. But the difficulty with Rice's hypothesis is that the temperatures required are too low. Also, on the basis of Rice's hypothesis, the outer planets (Saturn, Uranus, and Neptune) would show more striking colors than Jupiter, since their atmospheres are

much colder. In actual fact, the reverse is the case.

Papazian (1959) suggested that the color is induced in certain condensates by charged particle bombardment (as observed in the laboratory), might explain the Jupiter colors. The planet's atmosphere could be penetrated by 100-mev particles, which are fairly abundant.

3.2.2.1 Ammonia

Farkas and Harteck (1934) (mentioned by Wildt 1937) measured the stationary concentration of hydrogen atoms in decomposing pure ammonia and explained their results by the following secondary reactions

$$NH_3 + H \rightleftharpoons NH_4 \qquad (4)$$

$$NH_4 + NH_2 \rightarrow \begin{matrix} 2NH_3 \\ NH_3 + H_2 + NH \end{matrix} \qquad (5)$$

$$NH + NH \rightarrow N_2 + H_2 \qquad (6)$$

At room temperature Reaction 4 proceeded to the right. The experimental evidence suggested that at room temperature Reaction 5 proceeded three times faster than Reaction 6.

Earlier, Melville (1932) observed that in ammonia + hydrogen mixtures, the quantum yield of the photolysis of ammonia was drastically reduced by the addition of hydrogen. Farkas and Harteck suggested that this was because NH_2 and NH_4 were no longer present in approximately equimolal amounts, on account of the increased association of ammonia with the added hydrogen atoms; therefore, the NH_4 could enter into reactions such as

$$NH_4 + NH \rightarrow NH_3 + NH_2 \qquad (7)$$

Thus, Wildt (1937) suggested that the presence of hydrogen in large quantities could prevent the irreversible decomposition of ammonia. Wildt also mentioned that hydrazine (N_2H_4) could be an intermediate, but this is less likely, since hydrazine fluorescence (ammonia Schuster bands) has not been detected.

Lyman-α radiation at 1216 Å is an important contribution to photochemical processes. At this wavelength the Sun no longer radiates as a blackbody, but there is an intense emission line due to solar atomic hydrogen. Similar emission lines occur with less intensity at shorter wavelengths. Absorption in the wavelength region of 500 to 1100 Å is adequate for ionization. The following are examples.

$$NH_3 + h\nu \longrightarrow NH_2^+ + H + e^- \qquad (h\nu > 15.8 \text{ ev}) \qquad (8)$$

$$NH_3 + h\nu \longrightarrow NH_+ + H_2 + e^- \qquad (h\nu > 19.4 \text{ ev}) \qquad (9)$$

3.2.2.2 Methane

The photochemistry of methane has been studied by Mahan and Mandel (1962) by using the Krypton resonance line at 1236 Å. They obtained many compounds, of which the principal ones were hydrogen, ethane, propane, and acetylene and the secondary ones were methyl acetylene, normal butane, isobutane, ethylene, and propylene.

The basic reactions for the production of ethane (C_2H_6) are:

$$CH_4 + h\nu \longrightarrow CH_2 + H_2 \qquad (10)$$

$$CH_2 + CH_4 \longrightarrow C_2H_6^* \quad (11)$$

$$C_2H_6^* + M \longrightarrow C_2H_6 + M \quad (12)$$

(The asterisks refer to excited molecular states.)

Reactions between methylene (CH_2) and hydrocarbons are very fast, and Mahan and Mandel found that, in spite of very high light intensities, they could not cause the concentration of methylene radicals to become high enough for their combination to be important. Also, changing the light intensity by a factor of four did not change the acetylene-ethane ratio. Therefore they attributed acetylene formation to the exothermic (12 kcal/mole) reaction

$$CH_2 + CH_4 \longrightarrow C_2H_2 + 2H_2 \quad (13)$$

The formation of acetylene is exceedingly important because from it benzene can be obtained. Thus a whole range of aromatic compounds that could contribute to the observed colors in the Jupiter atmosphere would be available.

All the products of the photolysis of methane are subject to further photolysis. For example, ethylene (C_2H_4) can be produced as follows.

$$C_2H_6 + h\nu \longrightarrow C_2H_4 + H_2 \quad (14)$$

Absorption coefficients for several of the compounds have been measured, and in the vacuum ultraviolet they absorb very strongly (Ausl1oos et al.1964). According to Bonhoeffer and Harteck (Wildt 1937), neither H nor CH_3 react with surplus

CH_4. It was found that in a hydrogen atmosphere the formation of ethane was almost completely suppressed and the regeneration of methane proceeded via

$$CH_3 + H_2 \longrightarrow CH_4 + H \qquad (15)$$

Thus the abundance of methane over ethylene and other hydrocarbons in the atmosphere of Jupiter can be explained.

Sagan and Miller (1960) conducted corona discharge experiment in a 30:3:1 mixture of hydrogen, methane, and ammonia and analyzed the products by infrared and mass spectrometry. They positively identified C_2H_4, C_2H_6, C_2H_2, HCN, and acetonitrile. They state that acetylene could polymerize explosively under the conditions existing on the planet and produce compounds of high molecular weight, many of them highly colored.

Shapiro (1953) found that the brightness of Jupiter followed solar sunspot activity. This variation cannot be accounted for by the Sun's varying intensity, and it suggests some large-scale changes in the atmosphere.

Owen (1963) searched for spectral evidence of the presence of additional compounds in the Jovian atmosphere but found no traces. Table 9 summarizes his upper limits on these gases compared with current values for the abundances of the known atmospheric constituents.

Table 9

COMPOSITION OF THE JOVIAN ATMOSPHERE

(Best Current Values)

H_2	30-200 x 10^3 m atm
CH_4	150
NH_3	7
C_2H_2	< 3
C_2H_4	< 2
C_2H_6	< 4
CH_3NH_2	< 3
CH_3D	< 20
HCN	< 2
SiH_4	< 20
HD	< 500

He, Ne, and Ar expected but no specific tests for their presence have yet been made.

3.2.3 Spacecraft Measurements

There are at least three significant advantages in making measurements from a space probe rather than from the Earth.

First, there is no interference from the Earth's atmosphere.

Second, there is better angular resolution of radiation from Jupiter.

Third, there is the capability of observing emission spectra projected against the dark hemisphere of Jupiter. No

planetary emission lines have yet been unequivocally detected, since they are masked by the reflected sunlight. This is a crucial point, because substances present only in trace quantities can be detected from their emission in the ultraviolet but are not detected when absorption in the infrared only can be investigated, as in ground-based or satellite observations.

Exploitation of these three facets leads to the following experimental measurements.

(1) General spectral observation at wavelengths not accessible on the Earth in order to look for evidence of molecular species other than those already detected. For example, CH_3 absorbs at 2160 Å and lower. High spatial resolution may permit detection of local high concentrations of rare species.

(2) Emission spectra, especially microwave resonance emission and fluorescence. For example, ultraviolet absorption by ammonia leads to fluorescence from the NH formed in the photodecomposition. A problem here is the strong solar background, so that careful choice of wavelength is required.

(3) Particular spectral absorption and emission studies. By studying the character of the radiation emitted or absorbed by a particular species it is possible to obtain useful information on the structure of the atmosphere:

(a) Line broadening and shift. This is caused by pressure. The shift in microwave

resonance frequencies might be useful measurements. The shift is proportional to the magnetic or electric dipole moment of the molecule. Hence by observing an appropriate molecule, the pressure at its location in the atmosphere could be determined.

(b) Distribution of intensity in the rotational structure of molecular bands. This is influenced by temperature ordinarily. However, with photochemical reactions and collisions of the second kind, it is possible to populate molecules in particular states. Then the subsequent redistribution among the various possible states proceeds via radiative and collisional transitions and is, consequently, dependent on pressure.

These two examples show ways of obtaining information about the structure of the atmosphere. The radiation to be monitored must await further research, but many molecules would be suitable. For example, the microwave spectrum of ammonia has been studied extensively, so this molecule could probably be used for (a).

(4) Airglow. This is useful for studying reaction rates and is used extensively in the Earth's atmosphere.

(a) The detection, from the dark side of Jupiter, of radiation due to long-lived species, metastables etc. It is probable that this would be one of the best ways for detecting species present in small quantities only, since sunlight would be

absent. Helium and neon should also be detectable in this way.

(b) The detection of radiation from the shadow of one of Jupiter's satellites. This would allow short period changes in species concentrations to be studied and provide information on chemical reaction rates.

(c) Viewing from the dark side of the planet into the illuminated atmosphere. If the upper atmosphere is clear, the radiation received would be due to fluorescence and Rayleigh scattering. Spectral analysis would separate the two.

3.3 Atmospheric Temperature

3.3.1 Theoretical, Infrared, and Radio Wavelength Temperatures

The solid surface of Jupiter, if it exists, is not accessible to direct measurement from the Earth. Thus measured temperatures refer to the atmosphere above, at, or within the clouds. If there were no strong radiation belts, it would be possible to observe Jupiter at low microwave frequencies at which penetration of clouds and haze is optimum. As in the case of Venus, one would then expect to be able to detect thermal radiation from well below the visible cloud layers. However, any decimeter radiation from Jupiter is overwhelmed by the nonthermal component from the radiation belts. Determinations of temperature are therefore confined to radiometer measurements below 4 cm and to analysis of the fine

structure of the molecular bands that occur in the photographically accessible region of the spectrum.

A useful reference standard for the evaluation of temperature measurements is provided by the radiation equilibrium temperature of the planet. This temperature is the value that would be assumed by a perfect radiator having the dimensions and reflectivity of Jupiter and located at the same distance from the Sun. It can be evaluated by simply equating the incoming and outgoing radiation:

$$\pi R_J^2 \, (1 - A) E_J = 4\pi R_J^2 \, \sigma T^4 \qquad (16)$$

The left-hand side of equation (16) is the amount of absorbed radiation: the solar flux at Jupiter's distance from the Sun, E_J, absorbed by a planet with Jupiter's albedo, A, and the intercepted area of illumination πR_J^2. The right-hand side is the amount of emitted radiation: σ is the Stefan-Boltzmann radiation constant, T the temperature of the emitting body, and we assume rapid rotation so the planet emits over its entire surface area, $4\pi R_J^2$.

We assume that the emissivity of the planet is unity, which means that the temperature obtained from this calculation will be a lower limit. To obtain the maximum temperature, the factor 4 would be dropped to give the temperature of the subsolar point. Thus $T_{max} = \sqrt{2}\, T$. When the appropriate numbers are put into Eq. (16), we find

$$T = 93°K$$

$$T_{max} = 131°K$$

The true equilibrium temperature of the visible (illuminated) hemisphere will lie somewhere between these extremes, depending on considerations of the detailed reflecting properties (e.g., limb darkening) of the planet's surface. Low (1964) suggests a value of T = 124°K. It is important to realize that this value is independent of any atmospheric effects or any possible internal heat source (e.g., radioactivity) that the planet may contain. Since any combination of these two effects would tend to raise the mean temperature, the equilibrium value represents a minimum if these effects are present.

A summary of modern temperature measurements is presented in Table 10. At first glance, this table appears to present a bewildering array of temperatures. Some of the scatter is due to the intrinsic difficulty in the measuring process. However, some of the differences are undoubtedly a true reflection of the wavelength dependence of the atmospheric absorption coefficient.

Beginning with the shorter wavelengths, the temperatures determined from the hydrogen quadrupole lines are unreliable for two reasons. One, the extreme narrowness of the lines makes it difficult to determine the equivalent widths precisely. Two, even if this were possible, the work of Foltz and Rank (1963) suggests that these lines are strongly

Table 10

JOVIAN TEMPERATURE MEASUREMENTS

Temp. (°K)	Wave-length	Method	Identification & Central Wave-length of Relevant Absorber	Reference
170	0.83μ	Analysis of (3,0) H_2 quadrupole lines	H_2 0.83μ	Zabriskie 1962
120	0.83μ	Analysis of (3,0) H_2 quadrupole lines	H_2 0.83μ	Spinrad 1964
200 ± 25	1.1μ	Analysis of 3_3 CH_4 band	CH_4 1.1μ	Owen 1965
128 ± 2.3	9-13μ	Germanium bolometer	NH_3 10.5μ	Murray and Wildey 1963
150	.1 cm	Germanium bolometer	NH_3 1.28 cm	Low 1965
144 ± 23	.835 cm	Microwave radiometer	NH_3 1.28 cm	Thornton and Welch 1963
171 ± 20	3.03 cm	Microwave radiometer	NH_3 1.28 cm	Giordmaine, Alsop, Townes, and Mayer 1959
140 ± 38	3.13 cm	Microwave radiometer	NH_3 1.28 cm	Mayer, McCullough and Sloanaker 1958a, b
145 ± 18	3.15 cm	Microwave radiometer	NH_3 1.28 cm	Mayer et al. 1958a, b
173 ± 20	3.17 cm	Microwave radiometer	NH_3 1.28 cm	Giordmaine et al. 1959
193 ± 16	3.3 cm	Microwave radiometer	NH_3 1.28 cm	Bibinova, Kuz'min, Salmonovitch, and Shavlovskii 1962
189 ± 20	3.36 cm	Microwave radiometer	NH_3 1.28 cm	Giordmaine et al. 1959
200	3.75 cm	Microwave radiometer	NH_3 1.28 cm	Drake and Ewen 1958

the shadows of Satellites II and III in transit across the disk of the planet as compared to the general background. This increase corresponds to a temperature of 190°K or 160°K, depending on whether it is interpreted as coming from the umbra only or from the penumbra as well. Subsequent observations by Wildey (1965) failed to confirm this phenomenon and led him to the conclusion that it was variable in time. Low (private communication) was also unable to confirm the observation of hot shadows, but found isolated spots on the disk of the planet that were distinctly warmer than their surroundings.

A time variation has also been detected in the microwave region of the spectrum. The dominant absorber is again ammonia, which has a strong inversion transition at 1.28 cm. This absorption will be pressure-broadened in the Jovian atmosphere and has an intrinsically asymmetrical profile, rising steeply on the shortwave side, reaching its maximum and then tapering off gradually toward longer wavelengths (Cleeton and Williams 1934). Therefore observations of Jupiter's thermal radiation would be expected to show increasing temperatures with increasing wavelength separation from the absorption maximum (deeper atmospheric penetration). The values given in Table 10 appear to confirm this expectation in a qualitative way and are distinctly higher as a group than measurements in the 9 to 13μ region.

Alsop and Giordmaine (1961) have suggested that the difference between their measurements at 3.17 cm and those of

saturated, in which case they cannot be used for a simple temperature analysis. Thus the disagreement between the two determinations is understandable and reflects uncertainty in both the data and the method. It seems advisable to assign these determinations relatively low weight.

The analysis of the methane band at 1.1μ is based on only one plate and thus is uncertain. Its most noteworthy feature is the fact that even within its associated error range, it represents a relatively high value. If this value (or range of values) is accepted, it suggests a rather deep atmospheric penetration. At this wavelength, such a condition is not unlikely.

In the 9 to 13μ region, the atmospheric opacity is determined by a strong fundamental band of ammonia. As Kuiper (1952) has pointed out, the presence of this band means that temperatures measured in this region of the spectrum must refer to a level well above that of the visible clouds. This results from the fact that 1 cm atm of ammonia is opaque at these wavelengths, while the weaker bands (observed photographically) suggest an abundance of roughly 7 m atm in the Jovian atmosphere. In other words, at some wavelengths outside the 9 to 13μ region the light reflected by the planet has reached much lower levels of the atmosphere.

The thermal radiation received in the 9 to 13μ region is by no means constant over the disk. Murray, Wildey, and Westphal (1963) observed a large increase in radiation inside

Mayer et al. (1958a, b) at essentially the same wavelength may be real and may represent an effect of a visually observed disturbance in the cloud belt which occurred during the time of observation. In fact, Alsop and Giordmaine report an anomalously high value of temperature (268 $\pm$ 14°K) measured just after the observed disturbance occurred.

To summarize, it appears that there are significant temporal, spatial, and wavelength-dependent variations in the temperature of Jupiter's atmosphere. This should not be surprising, since we would observe the same general behavior if we were to examine the Earth from a vantage point outside its atmosphere. The temperature values in Table 10 are generally higher than the computed radiation equilibrium values. This has been interpreted as possible evidence for additional thermal radiation from Jupiter which is then envisaged as still cooling down from an early, high-temperature phase. However, recent work on the infrared spectrum of ammonia (Walsh 1963) suggests that this gas may have sufficient opacity in the appropriate region of the spectrum to provide a rather sufficient greenhouse effect. This means that visible radiation penetrating the planet's atmosphere would produce the warming corresponding to the radiation temperature. At this temperature (124°K), a body emits most of its energy near 23μ. Hence the ammonia makes the atmosphere relatively opaque, preventing the radiation from leaving and producing the required heating. Until more data on the ammonia spectrum and a better idea of

the possible influence of other absorbers are obtained, this interpretation must remain tentative.

3.3.2 Spacecraft Measurements

There are again three main advantages in making thermal measurements of Jupiter from a spacecraft. The first is the capability of observing at any wavelength desired. The second is the high angular resolution made possible by a close approach to the planet. The third is the capability of observing the unilluminated hemisphere.

The first advantage can, of course, be achieved by an orbiting telescope in the vicinity of the Earth. It is in utilizing this capability with the advantages of points two and three that a fly-by makes its great contribution. Such a mission would be able to accomplish the following objectives.

1. Search for variations in temperature at long (i.e., cloud-penetrating) wavelengths on the illuminated hemisphere. A correlation of such observations with ground-based studies of visible features in the cloud layer could contribute significantly to our understanding of the planet's circulation.
2. Obtain measurements of temperature at several wavelengths on both dark and light hemispheres to determine cooling rates and atmospheric heat capacity.
3. Extend the range of ground-based observations with high resolution to determine the wavelength-dependence of the atmospheric opacity and

possible variations over the disk due to temperature effects. Such measurements should help to determine whether a large atmospheric greenhouse effect exists.

3.4 Physical Aspects of the Clouds

3.4.1 Results from Polarization Studies

In comparison with polarization studies made on the terrestrial planets, Jupiter has received scant attention. This must be due, in part at least, to the small phase angles to which observations of Jupiter are confined ($< 11.7°$), compared with the larger angles available for the terrestrial planets (up to 47° for Mars).

Variation of polarization with phase angle is characteristic of many solid materials and aerosols of particular particle size and refractive index. Such variations have been used for elucidating the structure and the composition of the surfaces of Mars and the moon. Photometric measurements affect these determinations; in the spherical albedo the dependence of the phase integral on phase angle and wavelength is a function of surface composition and structure.

Polarization is defined with respect to the plane containing the source (Sun), the object (Jupiter), and the observer (Earth). $I_\perp$ and $I_\parallel$ are the intensities of the observed radiation components whose electric vectors are perpendicular and parallel to this plane, respectively. With this notation

the polarization, P, is:

$$P = \frac{I_{\perp} - I_{\parallel}}{I_{\perp} + I_{\parallel}}$$

In an atmosphere that contains only molecules

$$P = \frac{\sin^2 V}{2} \sec \theta \left(\frac{1}{\lambda}\right)^4 \text{constant}$$

where the sec θ term allows for the increased slant path through the atmosphere, and V is the phase angle. Of particular importance is the $(1/\lambda)^4$ law of wavelength dependence, because this provides the best test for a Rayleigh atmosphere (molecules only, or particles with diameter $\ll \lambda$). The polarization from a Rayleigh atmosphere is always positive. Polarization by aerosols can be positive or negative, depending on the particle size and refractive index. Furthermore, the variation with phase angle is quite characteristic (Dollfus 1961, van de Hulst 1957), but the wavelength dependence is less marked.

In a practical situation it is probable that there will be a mixture of particle sizes resulting in a polarization profile whose V-dependence is much less strong than that for one particular size. Consequently, the polarization profile is more difficult to interpret. In the case of Jupiter, the polarization of the light reflected by the clouds forms a background, and perturbations in the polarization curve are introduced by that part of the atmosphere above the cloud

layers. However, this situation will be dependent on the wavelength at which the observations are made, since the atmosphere above the clouds will have a more pronounced effect in the ultraviolet than in the infrared.

The polarimetric observations on Jupiter made before 1960 have been reviewed by Dollfus (1961), who is the major contributor to this field, the earliest work being performed by Lyot (1929). Lyot first measured the polarization of the central region of the disk as a function of phase angle. He found that the variation with phase angle changed slightly from 1923 to 1926, the polarization curve sometimes starting positive but turning negative at about V = 2° and falling to P = -0.006 at V = 11.7°. The differences from one year to the next could not be attributed to experimental error but may have been due in part to the different planetary longitudes involved. Variations across the disk were very slight until the edge was reached, when the polarization increased sharply (going positive).

Lyot also compared the polarizations of the bright equatorial zone and the dark belts adjacent to it. He found that they were usually very similar, although there were exceptions. The pole caps proved to have a completely different polarization. Lyot observed that the polarization of the grey areas was independent of phase angle. The direction of polarization was not the same at every point. Along the central meridian it was perpendicular to the meridian, and

away from this it became parallel to the nearest edge. Sometimes the characteristics of the polar cap extended nearer to the equator, with an ill-defined limit.

Recently Dollfus (1961) confirmed and extended Lyot's results. In particular, he measured the polarization of the bright zones flanking the equatorial plane in various wavelengths. The shapes of the polarization curves, plotted as functions of position across the disk, were very similar. They were fairly flat near the center and rose toward the edges, but not nearly so steeply as at the poles for a traverse along a meridian. The general shape showed some changes with phase angle. However, the individual bands did not show consistent differences, and the measurements established at the polarization depends but little on the darkness of the region or the spectral interval. The dependence was almost entirely on the position on the disk and on the phase angle. Dollfus confirmed the anomalous polarization in the polar regions.

The increase in the polarization at the limbs suggests a strongly scattering, transparent atmosphere. However, Lyot rejected this view because it requires that the light coming from the rims of the planet be polarized along a plane parallel to these rims, which condition is not found in the equatorial regions. He suggested that some other effect must be the cause, e.g., a decrease in cloud transparency when viewed obliquely. At the poles, however, a strongly scattering atmosphere, and no clouds, would be consistent.

Dollfus (1955, 1957) arrived at similar conclusions. His observations showed a comparatively small wavelength dependence, which did not fit a model atmosphere in which a dense cloud layer was covered by a pure gas. He found that his data could be interpreted as indicating that the atmosphere above the cloud layer contained thin veils, or mists. Calculations showed that consistency was obtained when these mists were composed of droplets of about 1μ diameter with a refractive index of 1.33. These veils should be weaker over the dark regions and disappear over the poles. Dollfus (1961) also reported that there was no appreciable wavelength dependence in the polarization of light from the poles and states that Ohman (1947) found the same.

Dollfus (1961) reported an interesting observation in 1924 (presumably made by Lyot) in which a grey cloud covered part of the north pole cap. The cloud showed negative polarization, similar to the center of the disk. The extent of the typical pole cap polarization was then limited to the regions not covered by the cloud.

In contradiction to Dollfus' results, Gehrels and Teska (1963) published data showing a distinct wavelength dependence of the polarization at Jupiter's poles and east limb.

3.4.2 Spacecraft Measurements

The discrepancies among the measurements made by different observers will probably be resolved fairly soon.

However, measurements from the Earth are limited to low phase angles ($<11°$), so that the interpretation of data is very difficult. Measurements of polarization from a fly-by probe can be expected to yield the major part of the polarization curve (the full curve would be 0° to 180°) and thus greatly facilitate interpretations. If the data are obtained with good resolution and in conjunction with photometric data, then an appreciable improvement in the knowledge of the atmosphere of Jupiter would result.

Drawing an analogy with Mars, which has been studied extensively by polarimetry,with good results, the best results would be achieved by taking measurements at the center of the disk and at the limb simultaneously. These would be made at a large number of wavelengths and over the available range of phase angles. The results would be expected to yield:

1. The nature of Jupiter's clouds, drop sizes, and constitution (ammonia crystals, liquid, methane, etc.)
2. The presence of veils, or mists, in the atmosphere above the clouds
3. The meaning of the zones and the belts and possible differences in their atmospheric compositions
4. The nature of the atmosphere over the poles
5. Data on the underlying structure, i.e., the deep atmosphere or the surface. Such data would be obtained if the polar regions have a fairly clear atmosphere free from aerosols.

Current knowledge of the polarimetric techniques is capable of this type of study but there is a lack of extensive laboratory experiments and theoretical studies needed to support such programs. During the next ten years, however, much of the necessary supporting work will surely be carried out.

Radar measurements might also yield information on the physical state of Jupiter's cloud layer, but weight and power requirements are more severe than for optical polarization measurements.

3.5 Ionosphere

An ionosphere on Jupiter has not been detected experimentally. However, in view of the known facts about the Earth's ionosphere, it would be difficult to explain the absence of a similar region on any planet having an atmosphere. It is known that the flux of X-rays and hard ultraviolet radiation from the Sun is absorbed in the Earth's atmosphere, with the consequent formation of the terrestrial ionospheric regions. Consistent with this theory, diurnal variations are observed and there is good correlation between increased solar activity (flares, sunspots, etc.) and onset of increased electron densities in the ionsphere.

The Earth's atmosphere is primarily composed of nitrogen and oxygen, and the ionospheric regions are formed through ionization of O and NO. Jupiter's atmosphere is primarily composed of hydrogen and helium, with smaller quantities of methane and ammonia. Laboratory data have shown that these molecules are also ionized by X- and ultra-

violet radiation; consequently it is improbable that there is no ionosphere of any kind on Jupiter.

3.5.1 Evidence from Decameter Radiation

Early observers of decameter radio emission believed that this phenomenon implied an ionosphere surrounding Jupiter. They believed that the source of the emission was either in or below the ionosphere and that the projection of the ionosphere strongly influenced the emitted radiation. As has been discussed in Section 3.1, some current opinion places the source of radiation emission well outside any ionospheric altitude, which would imply that the ionosphere is unconnected with this radiation. However, because of the historical development of the subject and because the results are quoted in other reviews, a brief review is given here of the deductions made from the decameter radiation observations.

Gardner and Shain (1958) suggested that the restricted frequency spectrum and its constancy over long periods of time (months) indicated a complete layer of ionization surrounding the planet. The spectral distribution and the observed circular polarization would indicate a plasma frequency of about 20 Mc. These authors suggested that the radiation might be due to plasma oscillations but offered no suggestions as to the cause. On this basis they estimated a collision frequency of ~ 2 sec^{-1}, as compared with 10^{-4} to 10^{-2} sec^{-1} for the terrestrial F-layer. Hence the pressure would be lower in Jupiter's ionosphere than in Earth's.

Gallet (1961) discussed the very small widths of the radiation bursts, remarking that they seem larger for 20 Mc than for 18 Mc. He pointed out that these effects can be readily interpreted on the hypothesis of a Jovian ionosphere, if the source of the radio emission is in or below the ionized region. His arguments concern the emission cone through the ionosphere, from a fixed source beneath it, and the effect of viewing this cone from Earth as Jupiter rotates on its axis. This postulate is in doubt.

Zhelezniakov (1958) considered the question from much the same point of view and also concluded that a plasma frequency of 20 Mc is implied. This plasma frequency implies a maximum electron density, n, of $5 \times 10^6/cm^{-3}$. This can be compared with the peak of Earth's F-layer, $10^6/cm^{-3}$. From the short duration of some of the bursts, the collision frequency, ν, has been estimated to be 10^2 to 10^3 sec^{-1}. Assuming that collisions are predominantly between charged particles, the effective collision frequency is:

$$\nu \cong 5.5 \frac{n}{T^{3/2}} \ln \left(220 \frac{T}{n^{1/3}}\right)$$

This gives a temperature, T, in the range 2000 to 20,000°K for an electron density of 5×10^6 cm^{-3}.

Using the theory for a Chapman layer with recombination at a temperature of 10^4°K, Zhelezniakov (1958) obtained a scale height of 1500 km for hydrogen molecules, a combination

rate of ~ 4 cm^{-3} sec^{-1}, and a recombination rate of $\sim 4 \times 10^{-14}$ cm^{-3} sec^{-1}. In this calculation it was assumed that each photon absorbed created an ion pair. As a comparison, the recombination rate for the terrestrial F-region is $\sim 10^{-10}$ cm^{-3} sec^{-1}, and the rate of electron production at the peak is ~ 200 cm^{-3} sec^{-1} and is ~ 400 cm^{-3} sec^{-1} at the peak of the E-region.

Rishbeth (1959) made similar calculations on the nature of a Jovian ionosphere, based on a plasma frequency of 20 Mc. He, too, used the Chapman theory but used a different temperature to estimate the scale height. Two temperature-composition models were selected. One considered a pure hydrogen atmosphere at 300°K, the other an atmosphere consisting of 63.5 percent hydrogen and 35 percent helium at 90°K. His results and those of Zhelezniakov are included in Table 11. The differences in the three models is small.

The deductions from theories assuming the observed decameter radiation originates below the ionosphere are on a somewhat shaky foundation, especially in view of the new results indicating the role of Io, which lies far above the ionosphere. As we shall see, however, direct theoretical treatments yield numbers in fair agreement with those given by the decameter studies, though peak electron densities are somewhat lower.

3.5.3 Theoretical Models

Zabriskie (unpublished) appears to have been the first

Table 11

IONOSPHERIC THEORIES

	Decameter Radiation			Theoretical Models			Terrestrial F-region (peak)
	Zhelezniakov	Rishbeth		Shimizu	Gross and Rasool		
		(a)	(b)		Model I	Model II	
Atmospheric composition	H_2	H_2 63.5% H He 35%		H_2 60% He 40%	H_2:He = 20:1	H_2:He = 0.03	Principally 0
Scale height, km	1500	10	100	8			300
Temperature, °K	10^4	90	300	130			
Density of neutrals at N_p, cm^{-3}	3×10^9 - 7×10^{10}	10^{12}	10^{10}	2×10^{10}	3×10^{13}	4×10^{13}	10^{10}
Density of H at N_p, cm^{-3}				2×10^{11}	3×10^9	4×10^9	
Altitude of N_p, km		Few hundred		170	210	110	280
Peak electron density n_p, cm^{-3}	5×10^6-10^7	5×10^6	5×10^6	10^7	7×10^5	10^6	2×10^6
Altitude of peak H conc., km				165	240	120	
Peak rate of production of electrons, q_p-cm^{-3} sec^{-1}	4	50	5		1	1	200
Altitude of q_p, km					350	160	180
Electron recombination rate	$< 4 \times 10^{-14}$*	$< 2 \times 10^{-12}$*		$< 5 \times 10^{-13}$*			5×10^{-9}**

* Radiative recombination

** Dissociative recombination

person to conduct a theoretical kinetic study of Jupiter's ionosphere. He included the effect of diffusion of hydrogen atoms but assumed an atmosphere of pure hydrogen and neclected the presence of helium. He found that the presence of negative ions had an appreciable effect on the electron density. Shimizu (1964) and Gross and Rasool (1964), however, omitted these particles.

Shimizu considered two atmospheric compositions: one of pure hydrogen, the other of 60% hydrogen and 40% helium. Shimizu points out that the dissociation cross section of hydrogen molecules by radiation in the Schumann-Runge region (1850 Å down to 1350 Å) is very small and may be less than 10^{-21} cm^2. Consequently, he used the following process for the dissociation of hydrogen:

$$H_2 + h\nu \ (< 804 \text{ Å}) = H_2^+ + e^-$$

$$H_2^+ + H_2 = H_3^+ + H$$

$$H_3^+ + e^- = 3\ H$$

He used a similar process invoking He^+. The production of electrons thus follows from the ionization of H, H_2, and He, and the removal by electron-ion recombination.

An essential prerequisite to making the computation on the ionosphere is the model atmosphere assumed. Apart from composition, which has already been given, Shimizu assumed a 2.8 atm pressure at the cloud top, a scale height of 8 km, and an isothermal atmosphere at 130°K. He further assumed

that diffusion was negligible and was then able to compute the absorption of solar radiation at various levels in the atmosphere. With these assumptions he solved the system of simultaneous differential equations (for H_2, H, H_2^+, H^+, H_3^+, e^- and also HeH^+, He^+, He for one model) and published profiles for H_2, H, and e concentrations. He did not discuss the solution of these equations, availability of rate constant data, etc. The results he obtained showed hardly any difference between the two model atmospheres. The electron density showed a peak of $\sim 10^7$ cm^{-3} at 165 and 170 km for the H_2/He and H_2 models, respectively, these being approximately the same altitude as the peaks in atomic hydrogen concentration. The number densities of atomic and molecular hydrogen were also about equal at this altitude.

Gross and Rasool (1964) used the same mechanism for the dissociation of hydrogen. They took two atmospheric compositions, H_2:He ratio (by volume) of 20:1 (from a review by Urey, 1959, and a ratio of 0.03:1 (Opik 1962). Their study shows mesopauses as 104 and 187 km for Model II (H_2:He = 0.03) and Model I (H_2:He = 20), respectively. For the exosphere they obtained temperatures of 135°K and 140°K for Models II and I, respectively.

In their calculation on an ionosphere, Gross and Rasool first estimated the distribution of atomic hydrogen, taking diffusion into account. For this they followed a method of solving the diffusion equation given by Zabriskie in 1960.

Their computations showed a maximum density of atomic hydrogen of 5×10^9 cm^{-3}, at an altitude of 10 to 20 km above the mesopause. The amount of atomic hydrogen was around 10^{-4} of the molecular hydrogen content, even at the peak (cf. Shimizu's approximate equality). Despite the large difference in the assumed compositions of the two models, the atomic hydrogen content was about the same. At sufficiently high altitudes atomic hydrogen predominated.

For their ionization equations Gross and Rasool clearly state their sources and the assumptions they make, which appear to be reasonable. Their resulting electron density profiles show electron density peaks at 120 km (Model II) and 230 km (Model I), with a second maximum on each curve on the high-altitude side. These maxima also appear in the curves for the rate of production of H^+. The peaks in the electron density profiles occur very close to the peak in the rate of ionization of H. The secondary maxima occur at the peaks in the rate of ionization of H_2. The peak electron densities were $\sim 5 \times 10^5$ and 10^6 electrons for Models I and II, respectively.

The results of the theories of Shimizu and of Gross and Rasool are also given in Table 11.

Zabriskie considered the various photo and kinetic reactions for hydrogen in considerable detail prior to making his computations for the ionosphere. He considered three atmospheric models: one consisting entirely of

molecular hydrogen, one consisting entirely of atomic hydrogen, and one consisting of both atomic and molecular hydrogen.

Applying the Chapman theory to the first model gave a peak electron density of 0.63×10^5 cm^{-3} and a gas density of 3×10^{10} cm^{-3}. The second model gave a similar result; the H^- ion was present in only very small quantities, because of efficient photo detachment, but was important through the reaction

$$H_2^+ + H^- \longrightarrow H_2' + H''$$

(the two neutral particles being excited in some way) which has a large rate constant. In the third model, Zabriskie computed the distribution of hydrogen atoms through the atmosphere by including diffusion processes. This gave much the same peak electron density as in the first model.

Zabriskie concluded that the major means of recombination was with H_2^+ and that the peak electron density could be appreciably more than 10^5 cm^{-3} if the assumed rate for this reaction were seriously in error. Both Gross and Rasool and Shimizu neglect this reaction altogether. Zabriskie also neglected helium in his computations, but thought this would have little effect unless it proved to be very abundant. He considered that methane might give rise to an electron density of around 10^4 cm^{-3} lower down in the atmosphere.

3.5.3 Assessment

From the point of view of making calculations to predict the structure of an ionosphere on Jupiter, it is fortunate that the neutral gases are hydrogen and helium. Rate constants for these molecules have been subjected to more theoretical scrutiny than any other molecules; experimental studies have also been extensive. Consequently many theoretical values for rate constants are available when experimental values are not.

Therefore, Gross and Rasool and Shimizu were able to include a large number of reactions in their treatments and their computations can be regarded with confidence. The figures they used for the solar flux were from rocket measurements published in 1961 and are probably quite accurate. Two likely sources of possibly large errors are (1) the simplified atmospheric models selected and (2) the neglect of effects of ambipolar diffusion of ions and electrons.

The results summarized in Table 11 demonstrate the agreement between the electron density values deduced from observations on decameter radiation and the values obtained through computation. However, it is important to note that these semiempirical deductions were made five to ten years ago, which is a long time in this rapidly advancing field. More recent theories (see Section 3.1.2) place the source of decameter radiation at distances that would be outside the ionosphere. If these are correct, the agreement shown in Table 11 between calculations and semiempirical deductions can

only be regarded as an interesting coincidence. It should also be stressed that Jupiter is known to have a large magnetic field. Consequently it is incorrect to neglect it when computing the electron density from a cutoff frequency, as was done in the papers cited.

Table 11 shows that the rate of production of electrons at the height of the peak electron density is probably a factor of 100 less than that for the terrestrial F2 region. The recombination coefficient is also much smaller, however, which accounts for the electron densities being comparable. Consequently, the decay rate must be less than that for the F2 region. This means that the diurnal variation is less on Jupiter, which effect will be accentuated somewhat by the shorter rotation period.

For Jupiter, the diurnal variation at the peak electron concentration can be expected to be small, perhaps negligible. For lower regions in Jupiter's ionosphere, this argument no longer applies. However, these regions are relatively much less accessible to observations from outside the planet's atmosphere than is the ionosphere above the peak referred to in Table 11.

Jupiter's atmosphere is known to contain appreciable quantities of ammonia and methane. These gases would, of course, form ionospheric layers also, if radiation of sufficiently high frequency were incident on them. Ammonia and methane will occur lower down in the atmosphere than hydrogen and helium.

Consequently the primary ionization will be as already described. There remains the possibility that some more ionized regions will occur further down in the atmosphere as a result of these gases. However, it is probable that they will be much weaker than the hydrogen and helium layers, because most of the solar ultraviolet radiation will have been absorbed.

3.5.4 Spacecraft Measurements

It would be desirable to determine ionospheric scale heights, densities of electrons and various neutral molecules, and dissociation and recombination rates. Unfortunately, not all these quantities can be measured directly by simple spacecraft passing far above the ionosphere.

An ionosonde experiment would provide a great amount of ionospheric data. Radio waves of various frequencies are beamed downward toward the planet. The time delay and the attenuation of the return signal are observed. Analysis is very much complicated by the presence of the Jovian magnetic field. However, experience with terrestrial topside ionosondes suggests that, with careful data reduction, we can obtain: (1) the electron density as a function of true height and (2) the electron collision frequency, also as a function of height.

Using these directly measured parameters, it may be possible to determine, from theory, the other ionospheric properties of importance, i.e., temperature, density of various molecular constituents, and dissociation and recombination rates.

The appropriate range of electron densities expected (see Table 11) is 10^5 to $10^7/cm^3$. This implies an ionosonde

frequency range of 3 to 30 Mc.

In order to obtain good return signals with modest transmitter power, a relatively close approach to Jupiter, $< 3\ R_J$, should be attempted.

A simpler experiment can determine ionospheric scale heights by the occultation of a radio frequency signal by Jupiter's ionosphere, as was done for Mare's ionosphere by Mariner IV. Because of a competing noise signal from Jupiter's decimeter radiation belt, low frequencies ($\sim$ 30-50 Mc) are probably required. A 40 R_J closest approach on a low-inclination flyby (to insure occultation) is adequate for satisfactory results, though closer approaches would increase precision.

3.6 The Interior of Jupiter

As a consequence of an obscuring cloud layer on Jupiter it is not possible to observe its solid surface, if one exists. Hence, theoretical models for describing the structure of the planet are proposed and then tested against the known mass, radius, and oblateness. In addition, observations of satellite motions can, in principle, yield the external satellite gravitational potential of the planet, although untangling satellite perturbations due to planetary gravitational potential within Jupiter from those due to mutual gravitational forces is very difficult.

The object of constructing a model that fits the observational data is to learn the following: composition, distribution of the various materials, pressure-density distribution, physical structure, and temperature distribution.

The first can be determined the best, the last cannot

yet be determined and the remainder are uncertain.

There are two major difficulties. First, the equations of state for possible materials are not known for pressures above 20,000 km, but the pressures of interest extend up to 10^7 atm or more. (Some isolated measurements may be possible up to 250,000 atm at the present time.) Second, the amount and the distribution of heavy materials is difficult to decide. Although these are present in small quantities, they can appreciably influence the gravitational moments.

According to De Marcus, if the equations of state for hydrogen and helium, the major constituents, were known exactly and if the exact pressure, density, and temperature of every level surface within the planet were known, the chemical composition of the planet still could not be deduced. It is possible to estimate the lower limit of the hydrogen content. It is apparent from the work reviewed here that assistance from theories of planetary evolution and measurements on the solar abundances of materials is still required to specify Jupiter's overall chemical composition.

Effective studies of this problem began in the 19th century with Airy and Darwin and were continued in this century by de Sitter, Jeffreys, Wildt, Ramsey, and others. The theoretical methods formulated by Darwin and de Sitter have been the basis for all subsequent computations. In 1958 De Marcus recast thie theory into a form that reduced the number of assumptions involved. On account of De Marcus' improvement in the computational method, new knowledge concerning the solar

abundances of the elements, and improved knowledge of the equation of state of hydrogen, this review has been confined to studying the work of De Marcus (1958) and Peebles (1964) and the reviews by De Marcus (1959) and Wildt (1961). In addition, brief mention is made of Ramsey's work (1951), which, though very important in the development of the subject, has been superceded by the later papers cited.

3.6.1 Method of Investigation

The procedure used to calculate the interior is to vary the density distribution, as suggested by physical considerations, until the geometrical ellipticity (measured by telescopic observations) matches the hypothetical ellipticity (perturbations in satellite motions imply a definite dynamic ellipticity of the surface for any postulated density distribution). The density distribution that satisfies the available tests gives a pressure-density relation for the materials of which the planet is composed. A study of the equations of state of likely materials, with abundance estimates (e.g., from solar abundances and mean planetary density) can then give a reconstruction of the deduced overall equation of state for the planetary material and determine the composition. The solution is not necessarily unique, however, and certainly depends on the extent to which the equations of state of likely materials are known.

In practice there is no distinct separation between these phases of the computations, as the constructed models are based on the probable compositions and equations of state

of the materials, i.e., the method is iterative by nature.

The earlier calculations, relying on the theory of de Sitter, were oriented toward determining the figure of a planet whose density distribution was known along some radius vector. De Marcus' great improvement was to depart from this requirement and provide a theory capable of finding the figure of the planet when only the equation of state of the material was known. The theory assumes hydrostatic equilibrium, i.e., the equipotential surfaces are also surfaces of constant density.

The external potential of the planet can be written as a series expansion in Legendre polynomials, with J and K denoting first and second moments. J and K, in turn, can be expressed in terms of two parameters ϵ and k, which express the ellipticity and the departure from the true ellipsoid shape, respectively. Measured and calculated ϵ and k are compared to test particular models.

Some assistance is also gained from several integral theorems propounded by Jeffreys, Chandrasekhar, and others. These give such quantities as mean pressure and an upper bound for the core pressure. Jupiter's core pressure must exceed 11.4×10^6 atm. Another theorem gives a bound to the surface density, ρ_1, as follows:

Jeffreys	$\rho_1 \leq 0.86$ gm cm^{-3}
De Marcus (from J)	$\rho_1 \leq 0.77$ gm cm^{-3}
De Marcus (from K)	$\rho_1 \leq 0.57$ gm cm^{-3} ,

(De Marcus used empirical values for J and K.)

3.6.2 Equations of State

As pointed out in Section 3.2, there is now no doubt that Jupiter is composed largely of hydrogen and that most of the remaining matter is helium. Consequently, it is for these two elements only that equations of state are required. Assuming that the density, ρ, is the density of a mixture of hydrogen and helium, then

$$\frac{1}{\rho} = \frac{\omega(H_2)}{\rho_{H_2}} + \frac{\omega(He)}{\rho_{He}}$$

where $\omega(H_2)$ and $\omega(He)$ are the mass abundances of hydrogen and helium, respectively. Peebles points out that if the material in Jupiter has roughly the same relative composition as in the Sun, then $\omega(H_2) \sim (2\text{-}3) \times \omega(He)$. Since $\rho_{He} \sim (2\text{-}4) \times \rho_{H_2}$, helium contributes only 10 to 20 percent of the total density. Consequently, an accurate knowledge of the equation of state for hydrogen is much more important than that for helium.

A thorough review of the equations of state for hydrogen and helium has been given by De Marcus (1958). The available experimental data are meager, especially at the high pressure involved. Therefore several attempts have been made to deduce the equation of state theoretically. Stewart (1956) has made measurements on solid hydrogen and helium at 4.2°K up to pressures of 20,000 atm. Since pressures up to 10^7 atm can be expected in the interior of Jupiter, the measurements do not cover all of the expected range of pressures.

There is considerable uncertainty about how matter behaves at very high pressures. The many different phases of ice observ ed by Bridgman is an example. In the present case extrapolation must be made to enormously greater pressures than have been achieved in the laboratory; explosive shock waves can generate pressures up to about 280,000 atm (Wildt 1961). It has been suggested by Wigner and Huntington (1935) that hydrogen may exist in a metallic form at very high pressures.

3.6.3 Jupiter Models

De Marcus began his calculations with a "zero temperature approximation" assuming pure hydrogen at 0°K. He found that the total mass contained within a sphere of radius r, M(r) did not approach zero as r approached zero, but was approximately 1/20 the mass of Jupiter. He therefore lumped this residue at the center in a "δ-function core". This model failed to give the correct moment of inertia. He then constructed a model comprising a mixture of hydrogen and helium in which the mass fraction of helium was chosen to be a monotomically decreasing function of radius. Again a δ-function was necessary to arrive at the correct mass. This model agreed fairly well with the observable external parameters shown in Table 12. These parameters were obtained from Brouwer and Clemence (1961).

De Marcus attempted to estimate the temperature in the interior of Jupiter but obtained a temperature of $\sim 10^4$°K at the base of the mantle (molecular region), and this was

Table 12

COMPARISON WITH ASTRONOMICAL DATA

	Observed	De Marcus	Peebles
Ellipticity, ϵ_1	0.0652	0.0645	
Departure from ellipsoidal shape, k_1	0.00052	0.00049	
First multipole moment J	0.02206 $\pm$ 0.00022	0.02130	0.025
Second multipole moment K	0.00250 $\pm$ 0.0014	0.00253	0.0027

inconsistent with the assumption of a solid mantle. He believes the internal temperature to be of the order of a few thousand degrees.

Ramsey and Miles also made careful calculations on the structure of the major planets. Ramsey (1951) considered a model with uniform hydrogen and helium concentrations (13 hydrogen atoms to 1 of helium), and later Ramsey and Miles (1952) included a δ-function core. Ramsey considered in considerable detail the overall composition and the distribution of component species in the major planets. He also discussed the equation of state for hydrogen, although not in the detail given by De Marcus. In his calculation he used the equation of state given by Kronig, de Boer, and Korriga, but added the zero-point energies. Ramsey assumes the planet to be solid throughout, consisting of molecular and metallic phases. He considers that the pressure of an atmosphere is of little importance so far as the bulk properties of the planet are concerned, even if a major part of the planet were gaseous, the equation of state of a gas at these pressures approximates that of a solid. He also treats the planet as being a uniform mixture of about 80 percent hydrogen and 20 percent helium.

Ramsey's work is obviously of great importance, but as far as the internal structure of Jupiter is concerned, De Marcus' work is more detailed, particularly concerning the upper region of the planet.

The general model assumed by Peebles was a high density, but not δ-function core surrounded by a uniform mixture of hydrogen and helium. For a given helium abundance he calculated the mass of the core necessary to yield the correct total mass and the two multipole moments, J and K. The radius of the core was chosen so that the pressure at the surface of the core was 8×10^7 atm (the limit of De Marcus' tabulations on the equation of state for helium). In order to investigate the dependence of hydrogen abundance on the helium distribution, a second set of models was studied in which the high-density core was replaced by a pure helium core, whose size was dictated by the need to keep the mass of the planet fixed.

Peebles used seven models:

1. Cold planet, T = 0°K
2. Isothermal atmosphere, T = 150°K
3. Adiabatic atmosphere, T = 150°K at 5 atm
4. Adiabatic atmosphere, T = 150°K at 1 atm
5. Adiabatic atmosphere, T = 150°K at 1 atm, using the lower density extrapolation of Stewart's results
6. Cold planet, using the lower density extrapolation of Stewart's results
7. Adiabatic atmosphere, T = 150°K at 3 atm.

The calculations were performed for various number ratios of hydrogen to helium in the mixture outside the core, and the results were compared with the astronomical data.

The assumptions about the atmospheric conditions were based on a temperature in the region of 150°K at the top of the cloud layer, with a pressure in the range of 1 to 5 atm. It was possible to obtain the observed value of J with models 1 to 14 and 7 by selecting an appropriate helium abundance. It would also be possible for the least dense atmosphere (model 5) if the helium were assumed to be concentrated toward the outer layers of the planet. The quoted errors in the observed value of K were such that all models would fit; hence this was no use as a test. For models that fit, it was found that the hydrogen abundance ranged from 0.85 for a completely cold planet of uniform composition to 0.70 for a deep adiabatic atmosphere with all the helium and heavy elements concentrated at the center.

Peebles found that the observed moment, J, for Jupiter could be obtained by assuming either a very deep or a very shallow atmosphere. But for a shallow atmosphere the hydrogen abundance in the upper layers would have to be very large, with a mass fraction ~ 0.9, unless the density of hydrogen were 25 percent less than he assumed in his calculations. This would be hard to explain, since it exceeds the estimated abundances in the Sun, obtained by various means. From consideration of the origin of the planets (Kuiper 1952), it appears that the protoplanets may have had cores of heavy elements (Si, Fe, O, etc.) amounting to as much as 0.3 percent of the total mass.

Peebles estimates that the gravitational separation of volatile elements, assuming a temperature around 10^4°K, would have a characteristic time of 10^{13} years. In addition, after Jupiter achieved its present state, the time for a helium atom to diffuse the distance of a planetary radius would greatly exceed the age of the solar system. Peebles concludes that the hydrogen in the surface layers of Jupiter should not exceed the solar abundance and, consequently, the planet has a deep adiabatic atmosphere. Hence, Peebles selects model 7, which gives the conditions, within errors, of the top of the cloud layers and which is also consistent with a model for Saturn.

The pressure density relation for this model is given in Figure 9 for comparison with other models. In this model the mass fractions were obtained by assuming that the volatile part of the heavy elements was 2 percent by mass originally. Hence the mass fractions in the region above the core are:

Hydrogen	0.80
Helium	0.18
Heavy elements	0.02

In his calculations, the heavy elements were treated like helium; the error introduced was negligible. The core for this model amounted to 2 percent of the total mass.

In conclusion, there is general agreement that Jupiter must be composed mainly of hydrogen, with some helium and a smaller amount of heavy elements. The hydrogen abundance is

FIGURE 9
MODEL DENSITIES OF INTERIOR

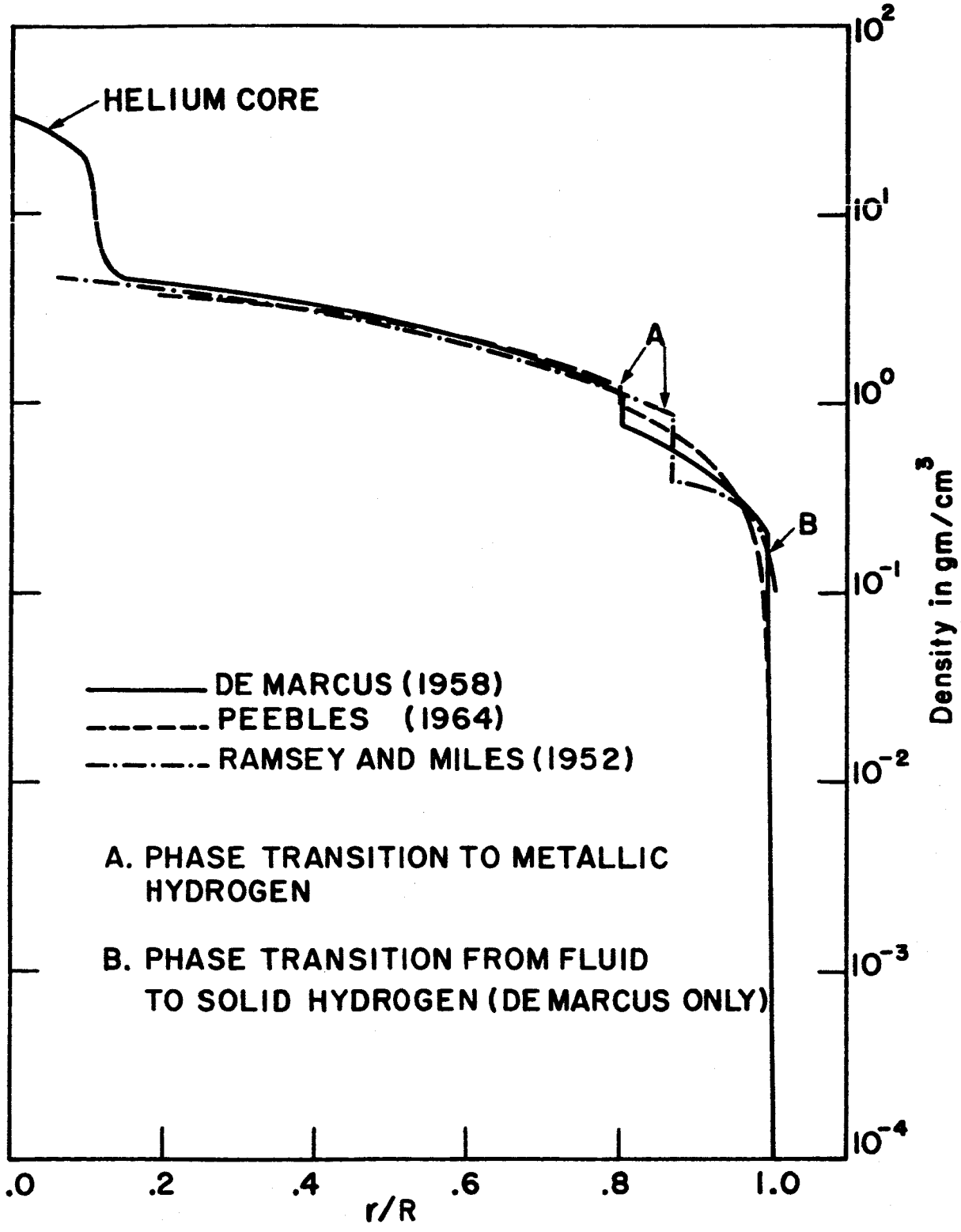

generally believed to be 75 to 80 percent by mass. The heavy elements are possibly about 2 percent, but this figure is uncertain. The remainder is helium. Ramsey and Peebles believe the planet consists of a homogeneous mixture of hydrogen and helium outside the core, whereas De Marcus believes there is an increase in the concentration of helium at smaller radii. Ramsey and Peebles support their model by considering the times required for gravitational separation in the planet and the pressure occurring in the protoplanet.

The presence of a dense core of heavy elements was necessary in many models to give the correct mass for the planet. In Peebles' model, however, a slight increase in the density of hydrogen would remove the necessity for such a core, and the model of De Marcus behaved the same way. Since the structure at the center of the planet cannot influence the gravitational moments at the surface, there appears to be no way of testing theories about this region. Instead, one must rely on theories of the origin of the solar system and planets to provide the answer.

Figure 9 shows the three models. The phase transitions were not identified explicitly by the authors, but they must be as indicated. It is not at all surprising that all three models agree in the region of metallic hydrogen, since they are all based on the same or similar (Ramsey and Miles) equation of state. Peebles makes no statement about the transition to solid hydrogen from the fluid state, so that one is left with

the impression that the phase change is directly from fluid to metallic hydrogen. De Marcus includes some solid hydrogen but states that the fluid state might persist up to the transition to the metallic phase.

As in the ionospheric studies, results tend to agree, even though the assumptions differ. Although there may be significant physical differences among the models used to derive the data in Figure 9, the actual density distribution probably lies near the curves shown there.

3.6.4 Spacecraft Measurements

A spacecraft on a fly-by mission to Jupiter does not actually reach the interior. Even so, the interior can "reach out" to produce measureable effects.

No experiment in Table 1 is directly oriented toward studies of Jupiter's interior, but some are relevant. One characteristic of the interior is its electrical conductivity, which can act as a bounding parameter for model interior studies. Field, Hyde, and Jamieson (1965) have suggested that measurements of the magnetic field near Jupiter, Experiment 1 of Table 1, might be useful in obtaining conductivity profiles.

The composition of the atmosphere also serves as a boundary condition for the model studies. Experiments 7 and 8 can measure this composition much more accurately at present. In particular, the hydrogen and helium abundance, which are parameters of great importance for model studies, would thus be better determined.

REFERENCES

Alsop, L. and Giordmaine, J. A. 1961, Columbia Radiation Laboratory Special Technical Report AD 263 565.

Ausloos, P., Gorden, R., Lias, S. G. 1964, J. Chem. Phys. 40, 1854.

Baum, W. A. and Code, A. D. 1953, Occultation Observation, A. J., 58, 108.

Berge, G. L. 1964, "The Brightness Distribution of Jupiter's 10 and 21 cm Radio Emission" (presented at the 117th meeting of the American Astronomical Society, Montreal, December.

Berge, G. L. and Morris, D. 1964, Ap. J., 140, 1330.

Bibinova, V. P., Kuzmin, A. D., Salomonovich, A. F., and Shavlovskii, I. V. 1962, Astr. Zhur. 39, 1083.

Bigg, E. K. 1964, Nature, 203, 1008.

Brouwer, D., and Clemence, G. 1961, Chapter 3 in "Planets and Satellites" Edited by G. P. Kuiper and B. M. Middlehurst, Chicago Univ. Press.

Cadle, R. D. 1962, J. Atmos. Sci. 19, 281.

Chang, D. B., and Davis, L. Jr. 1962, Ap. J., 136, 567.

Cleeton, C. E. and Williams, N. H. 1934, Phys. Rev. 45, 234.

Davies, W. O., Narin, F., Roberts, D. L., Schmidt, L. A., Scholz, L. C., Stone, C. A., and Vickers, R. 1964, ASC/IITRI Report M-1, "Survey of a Jovian Mission".

De Marcus, W. C. 1958, Astron. J. 63 (1), 2.

De Marcus, W. C. 1959, "Planetary Interiors", Handbuch der Physik LII, 419.

Dollfus, A. 1957, "Study of the Planets by Means of the Polarization of their Light", Thesis, University of Paris, May 21, 1955, NASA TT F-188, July 1964, Suppl. Ann d'Astrophys. 4, 1-114.

Dollfus, A. 1961, "Polarization Studies of Planets", Chapter 9 in Planets and Satellites, Edited by G. P. Kuiper and B. M. Middlehurst, University of Chicago Press.

Dowden, R. L. 1962, J. Geophys. Res. 67, 1745.

Drake, F. D. and Ewen, H. I. 1958, Proc. I.R.E., 46, 53.

Dulk, G. A. 1964, "Influence of the Satellite Io on the Decametric Radio Emission from Jupiter", presented at the 117th Meeting of the American Astronomical Society, Montreal.

Dulk, G. A. and Gordon, M. A. 1965, High Altitude Observatory Report at Conference of Decameter Burst Observers, Greenbelt, Maryland, April.

Ellis, G. R. A. 1962, Aust. J. Phys. 15, 344.

Ellis, G. R. A. 1963a, Aust. J. Phys. 16, 74.

Ellis, G. R. A. and McCulloch, P. M. 1963b, Aust. J. Phys. 16, 380.

Farkas, and Harteck, P. 1934, Z. fur Phys. Chem. B25, 257.

Fermi, E. 1949, Phys. Rev., 75, 1169.

Field, G. B. 1959, J. Geophys. Res. 64, 1169.

Field, G. B. 1960, J. Geophys. Res., 65, 1661.

Field, G. 1965, in "Hydrogen Molecules and Astronomy: A Review", Princeton University.

Field, G. B., Hide, R. and Jamieson, J. C. 1965, private communication.

Foltz, J. V., and Rank, D. H. 1963, Ap. J. 138, 1319.

Gallet, R. M. 1961, "Planets and Satellites" Edited by G. P. Kuiper and B. M. Middlehurst, Chicago University Press, Chapter 14.

Gardner, F. F., and Shain, C. A. 1958, Aust. J. Phys. II (I), 55.

Gehrels, T., and Teska, T. M. 1963, Appl. Optics, 2, 67.

Giordmaine, J. A., Alsop, L. E., Townes, C. H., and Mayer, C. H. 1959, A. J. 64, 332.

Gross, S. H., and Rasool, S. I. 1964, Icarus, 3, 311-322.

Kerr, F. J. 1962, Sky and Telescope, 24, 254.

Kiess, C. C., Corliss, C. H., and Kiess, H. K. 1960, Ap. J. 132, 221.

Kuiper, G. P. 1952, Atmospheres of the Earth and Planets, Edited by G. P. Kuiper, University of Chicago Press, Chapter 12.

Low, F. J. 1961, Opt. Soc. America, 51, 1300.

Low, F. 1964, Astron. J. 59, 550.

Low, F. 1965, private communication.

Lyot, B. 1929, "Research on the Polarization of Light from Planets and From Some Terrestrial Substances", Annales de L'Observatoire de Paris, Section de Meudon, Vol. VIII, No. 1, NASA TT-F-187, July 1964.

Mahan, B. H., Mandal, R. 1962, J. Chem. Phys. 37, 207.

Mayer, C. H., McCullough, T. P., and Sloanaker, R. M. 1958a, Ap. J., 127, 11.

Mayer, C. H., McCullough, T. P., and Sloanaker, R. M. 1958b, Proc. I.R.E., 46, 260.

Morris, D. and Berge, G. L. 1962, Ap. J., 136, 276.

Melville, 1932, Trans. Far. Soc. 28, 885.

Morrison, B. L. 1962, US Naval Obs. Circular No. 92, Washington.

Murray, B. C., and Wildey, R. L. 1963, Ap. J. 137, 692.

Murray, B. C., Wildey, R. L., and Westphal, J. A. 1964, Ap. J. 139, 986.

Ohman, Y. 1947, Stockholm Osv. An. 15, No. 2.

Opik, E. J. 1962, 11th International Astrophysical Colloquium, Liege, July 1962, Mem. Soc. Roy. Sci. Liege VII, 47. Also, Icarus 1, 200, 1962.

Owen, T. C. 1963, PASP, 75, 314.

Owen, T. C. 1965, Ap. J., 141, 444.

Papazian, H. A. 1959, PASP, 71, 237.

Peebles, P. J. E. 1964, Astrophys. J. 140 (1), 328.

Peek, B. M. 1958, "The Planet Jupiter", Macmillan.

Radhakrishnan, V., and Roberts, J. A. 1960, Phys. Rev. Letters, 4, 493.

Ramsey, W. H. 1951, Mon. Not. Roy. Astron. Soc., London, 111, 427.

Rank, D. H., Fink, U., Foltz, J. V., and Wiggins, T. A. 1964, Ap. J. 140, 366.

Rice, F. O. 1956, J. Chem. Phys. 24, 1259, and "The Chemistry of Jupiter", Scientific American, 1956.

Rishbeth, H. 1959, Austr. J. Phys. 12 (4), 466.

Roberts, D. L. 1964, ASC/IITRI Report P-1, "The Scientific Objectives of Deep Space Investigations - Jupiter".

Roberts, J. A. 1963, Planetary and Space Sci., 11, 221.

Sagan, C., and Miller, S. L. 1960, A. J. 65, 499.

Shapiro, R. 1953, J. Meteorology 10, 350.

Shimizu, M. 1964, Progr. of Theor. Phys. 32 (6), 977.

Smith, A. G. and Carr, T. D. 1963, Radio Exploration of the Planetary System, Van Nostrand, Princeton.

Smith, A. G., Lebo, G. R., Six, N. F. Jr., and Carr, T. D. 1965, Ap. J., 141, 457.

Spinrad, H. 1964, App. Optics, 3, 181.

Spinrad, H. and Trafton, L. 1963, Icarus, 2, 19.

Stewart, J. W. 1956, J. Phys. Chem. Solids, 1, 146.

Thornton, D. D. and Welch, W. J. 1963, Icarus, 2, 228.

Urey, H. C. 1959, "The Atmospheres of the Planets" Handbuch der Physik LII, p. 407.

Urey, H. C. and Brewer, A. W. 1957, Proc. Roy. Soc., A241, 37.

Walsh, T. E. 1963, Prog. Report ONR Contract NONr 2481 (58) Johns Hopkins University.

Warwick, J. W. 1961, Annals New York Acad. Sci., 95, 39.

Warwick, J. W. 1963a, Ap. J., 137, 41.

Warwick, J. W. 1963b, Ap. J., 137, 1317.

Warwick, J. W. 1964, Annual Review of Astronomy and Astrophysics, 2, 1.

Warwick, J. W. and Dulk, G. A. 1965, "Observation of Jupiter's Sporadic Radio Emission in the Range 7.6-41 Mc/s January 1964 through May 1965", High Altitude Observatory, Boulder, Colorado.

Wigner, E. P. and Huntington, H. B. 1935, J. Chem. Phys. 3, 764.

Wildey, R. L. 1965, J. Geophys. Res., 70, 3796.

Wildt, R. 1932, Veroff. U. Sternw. Gottingen 2, Heft 22, 171.

Wildt, R. 1937, Ap. J. 86, 321.

Wildt, R. 1961, "Planetary Interiors", Chapter 5 in Planets and Satellites, Edited by G. P. Kuiper and B. M. Middlehurst, Chicago University Press.

Zabriskie, F. 1962, A. J., 67, 168.

Zhelezniakov, V. V. 1958, Sov. Astr. 2 (2), 206.